TÉCNICO LISBOA

Model-driven catalyst design for ethanol dehydration into ethylene

Diogo Rafael Teixeira de Ascensão

Thesis to obtain the Master of Science Degree in

Chemical Engineering

Supervisors: Prof. Dra. Carla Isabel Costa Pinheiro
Prof. Dr. Ir. Joris Thybaut

Examination Committee

Chairperson: Prof. Dr. Carlos Manuel Faria de Barros Henriques
Supervisor: Prof. Dra. Carla Isabel Costa Pinheiro
Member of the Committee: Prof. Dr. Pedro Simão Freitas Mendes

October 2022

”A positive mindset brings positive things”

Acknowledgments

Firstly, I would like to thank my coaches Ana Bjelič and Jeroen Poissonnier for all the help and guidance during the development of this master thesis and for always being open to having meetings and giving a hand when needed. To Carla Pinheiro, my IST supervisor for all the tips and recommendations given to me along this process. I would also like to thank professor Joris Thybaut, my U. Gent supervisor for the remarks done during the presentations and discussions that we had.

Secondly my friends. I would like to thank Duthoit and Bernardo for coming along with me on this journey of doing my master's thesis abroad, and for always having my back especially when things were harder. A big thank you also to Alexandrina, Inês and Maria Ana for these amazing 5 years of work, reports, and projects. You definitely made these years worthwhile and easier to go by with all the good moments we have had together.

To my oldest friends Cunha and Tiago, a big thank you as well. Even though being apart from each other for the majority of the 5 years, you always had the gift of knowing when things were not going so well and doing things to help me keep my head up.

I would also like to thank all the people involved in my stay in Belgium for making me feel welcome and being always available to help me.

To my loved one, Adriana, thank you so much for never doubting me and my capabilities. Thanks to you and your words of encouragement, I overcame all the difficulties and hard times that appeared along the way. You became not only my girlfriend but also the biggest supporter I could have asked for.

Por último, não posso deixar de agradecer à minha família. Aos meus pais Fernando e Cristina, o meu maior obrigado. Sei que este objectivo era tanto meu como vosso e concretizá-lo não seria possível sem o vosso apoio incondicional. Agradeço também aos meus avós Orlando, Celeste e Crisanta por toda a disponibilidade e preocupação demonstrada ao longo de todo o meu percurso como estudante.

Abstract

Olefins, mainly produced by steam cracking, are playing a bigger part in the chemical industry, year by year. However, with the rise in environmental awareness and the new environmental policies, the search for greener production processes is very important. Dehydration of ethanol into ethylene, the process of interest in this thesis appears as one of the main alternatives to this problem. However, the ideal catalyst for this is yet to be found. Hence, a methodology previously developed, named ”Model-driven catalyst design”, was applied in this work to identify the most suitable catalyst properties to maximize ethylene yield. This methodology integrates the kinetics of the process, by using identified catalyst descriptors, namely chemisorption enthalpies, sticking coefficients and active site density, with statistical tools. It has as main objective to establish relationships between catalyst properties and the observed performance. Experimental data reported in two different studies obtained over zeolite-based catalysts modified through dealumination and metal doping processes, with phosphorous and lanthanum, were used in this work to correlate catalyst physical properties with their catalytic activity. Obtained relationships show that lower chemisorption enthalpies of ethylene are associated with good performances while higher values are related to worst performance selectivity-wise. This appeared associated with catalysts doped with phosphorous, which leads to modifications in the catalyst's porous structure and in the acidity of the catalyst. Yet, this constitutes preliminary conclusions and broader datasets should be studied in the future, so getting to an optimal catalyst composition can be an easier process.

Keywords

Catalyst descriptor, Kinetic modelling, Ethylene, Dehydration, Catalyst design, Virtual Catalyst

Resumo

Olefinas, maioritariamente produzidas através de *steam cracking*, estão a tornar-se cada vez mais relevantes para a indústria química com o passar dos anos. Contudo, com o aumento da consciência ambiental e de novas políticas ambientais, a procura por processos mais sustentáveis torna-se importante. A desidratação de etanol a etileno, o processo de interesse para esta tese, é considerada uma das principais alternativas para este problema. Todavia, ainda é necessário encontrar o catalisador ideal. Assim, neste trabalho foi aplicada uma metodologia previamente desenvolvida, denominada *"Model-driven catalyst design"*, para identificar as propriedades do catalisador mais adequadas para aumentar o rendimento em etileno. Esta metodologia integra a cinética do processo, ao utilizar descritores catalíticos identificados, como entalpias de quimissorção, *sticking coefficients* e a densidade de centros ativos, com ferramentas estatísticas, tendo como objetivo estabelecer relações entre as propriedades do catalisador e a performance observada. Dados experimentais reportados em dois estudos obtidos sobre zeólitos modificados através de processos de desaluminação e *doping* metálico, com fósforo e lantâno, foram utilizados neste trabalho para correlacionar as propriedades físicas do catalisador com a sua atividade. As relações obtidas mostram que valores mais baixos de entalpia de quimissorção de etileno estão associados com boas performances enquanto valores mais altos estão ligados a pior performance em termos de seletividade. Isto surge associado a catalisadores dopados com fósforo, modificando a estrutura porosa e a acidez do catalisador. Contudo, estas conclusões são preliminares e devem ser realizados estudos com dados experimentais mais vastos, para facilitar a obtenção de um catalisador ótimo.

Palavras Chave

Descritor catalítico, Modelação cinética, Etileno, Desidratação, Design catalítico, Catalisador virtual

Contents

List of Figures

List of Tables

Acronyms

DAE	Differential Algebraic Equation
DEE	Diethyl Ether
DFT	Density Functional Theory
DoE	Design of Experiments
ER	Eley-Rideal
EIA	Energy Information Agency
FFF	Fast Flexible Filling
FTS	Fischer-Tropsch synthesis
LHHW	Langmuir-Hinshelwood-Hougen-Watson
LPG	Low Pressure Gas
MtO	Methanol to olefins
MDCD	Model-driven catalyst design
OCM	Oxidative Coupling of Methane
ODH	Oxidative dehydrogenation of light alkanes
RDS	rate determining step
SC	steam cracking

1

Introduction

Contents

1.1 Introduction

With a claimed production capacity of 200 million tons by 2024 and a predicted increase of almost 40% for the decade between 2016 and 2026, ethylene is one of the chemicals with the largest production in the world, being not only an important product but a very important raw material, or intermediate, for the production of several products, such as acetic acid and styrene [1].

The conventional processes for the production of ethylene rely majorly on fossil fuels, since the main production route for it is steam cracking. However, due to the rise of environmental concerns and the demand for this fuel, finding new ways to produce this kind of product is a priority [2, 3].

Among many processes like Methanol to olefins (MtO), Oxidative Coupling of Methane (OCM) or Fischer-Tropsch synthesis (FTS), ethanol dehydration to ethylene is reported to be one of the best alternatives, especially with the rise of bioethanol production, and the ease how this can be produced from biomass [2]. However, for this process to be viable more insights and search needs to be done, especially regarding the operating conditions and catalyst.

There are three types of catalyst development techniques, statistics-driven design, performance-driven design and information-driven design. There is also an emerging approach related to information-driven design, entitled Model-driven catalyst design (MDCD) hereinafter, which is based on the concept of catalyst descriptors [4].

1.2 Objectives

The objective of the present work was to apply the MDCD to identify the properties of zeolite-based catalysts that largely affect ethanol conversion and ethylene selectivity and therefore provide guidelines for the catalyst synthesis

To this end, a kinetic model based on the reaction mechanism and catalyst descriptors was developed considering an ideal plug flow reactor. Various virtual catalysts, defined by a combination of the descriptor values (which will be defined after), were formulated and tested *in silico* with the developed kinetic model.

The performance of virtual catalysts was compared with one of the real catalysts and the match was statistically evaluated to establish relationships between the physical properties and observed performance, aiming to find a catalyst composition that would provide, maximal yield and selectivity of ethylene.

1.3 Outline

The thesis is divided into 6 different chapters.

The chapter 1 is related to the short introduction and objectives of the thesis already presented earlier. Chapter 2, consists of: i) a review of the ethanol dehydration to ethylene process, focusing on the reaction mechanism and, tested catalysts and ii) an introduction to new catalyst development techniques. In chapter 3 the procedure followed for the MDCD is explained. Chapter 4 provides a discussion on results obtained by applying MDCD methodology to the ethanol dehydration to ethylene making use of the experimental data from two different case studies.

Finally in chapter 5 conclusions on the developed work are taken, followed by some suggestions for future work in chapter 6.

2

Literature Survey

Contents

2.1 Market

2.1.1 Ethylene

Ethylene, or Ethene, is the most simple olefin that exists and is one of the major building blocks in the chemical industry. It became this important during the 1940s when American oil and chemical companies started to produce it from refinery byproducts like ethane or natural gas, through a steam cracking (SC) process [5].

Another event that strongly influenced ethylene production was the Second World War because associated with it a huge growth in petrochemistry and the petrochemical area was observed. Two principal factors appeared connected to this growth and had a role in this time: the first one is associated with an increase in the demand for gasoline, where ethylene and other olefins can be used as additives to improve fuel quality. The second factor was discovering and improving the processes that convert olefins into more useful chemical products [6].

Since the times of the Second World War, mainly due to its high reactivity, ethylene became one of the largest volume building blocks for petrochemical production, being the raw material for the production of around 25% of this chemical area, and one of the most produced chemicals in the world [7]. Consequently, ethylene has a very big value chain around it, being a feedstock for the production of important chemicals like acetic acid, ethylene glycol, ethylbenzene, styrene, and polyethylene as Figure 2.1 shows [1, 8].

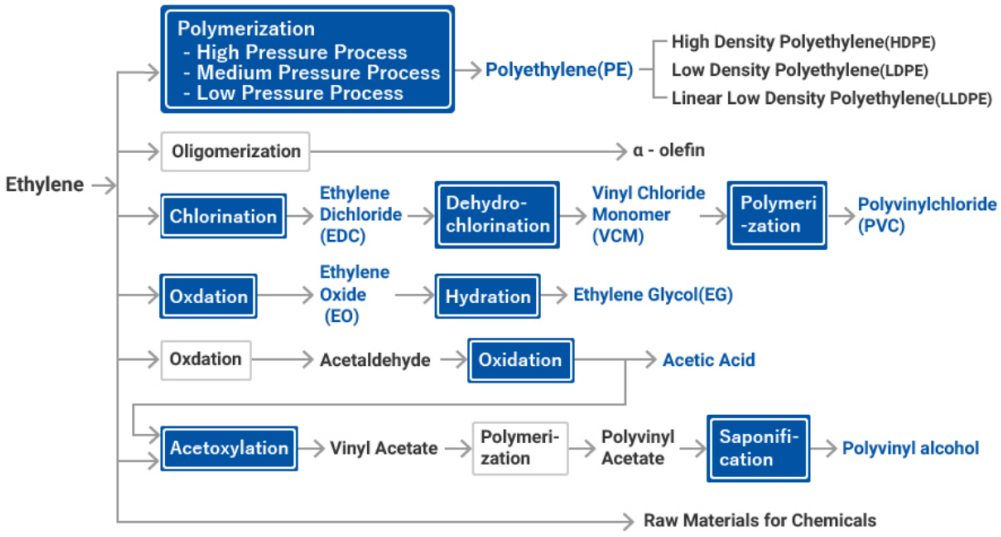

Figure 2.1: Ethylene derivatives value chain [9].

Marketwise, ethylene is a commodity that can be considered as a measure of a country's economy, since growth or decrease in the petrochemical sector income is directly correlated with a country's econ-

omy. This, associated with a constant demand for petrochemical products will lead to an increase in the production capacity of ethylene over the years according to [1].

Figure 2.2, demonstrates among other world base chemicals, that ethylene production capacity will reach around 200 million metric tons by the year 2024 [1].

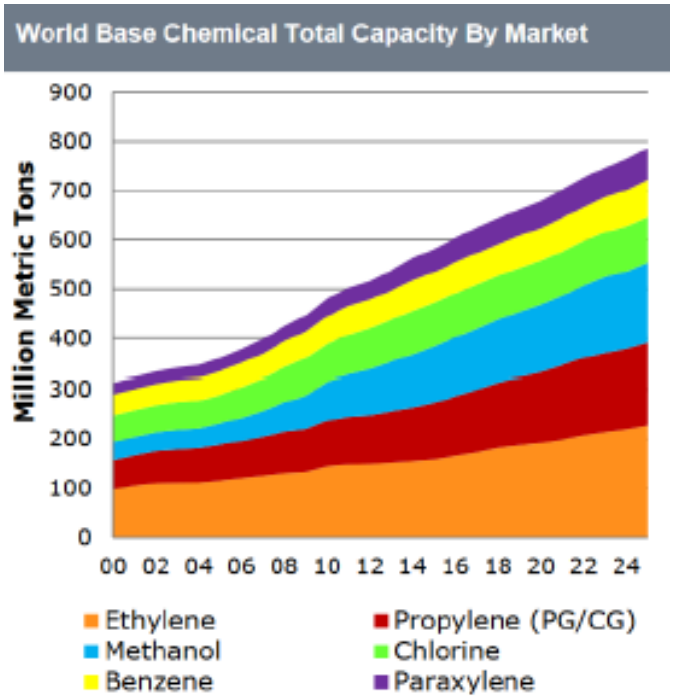

Figure 2.2: Forecast for the global chemical capacity including ethylene [1].

Furthermore, a rise of about 39% is reported for the decade between 2016 and 2026, principally associated with the rise of the economy and consumption levels in areas like China and the Middle East, indicated in Figure 2.3 [1]. On top of this, the increase in the world's population and also its living standards can play a big role in this increasing trend.

Due to this rise in the demand for fossil fuels and petrochemical derivatives, and the constant rise of environmental awareness by the population, a continuous search for alternative and more sustainable processes and feedstocks for ethylene production will be required, in order to decrease the dependency on fossil-based ones [1, 8].

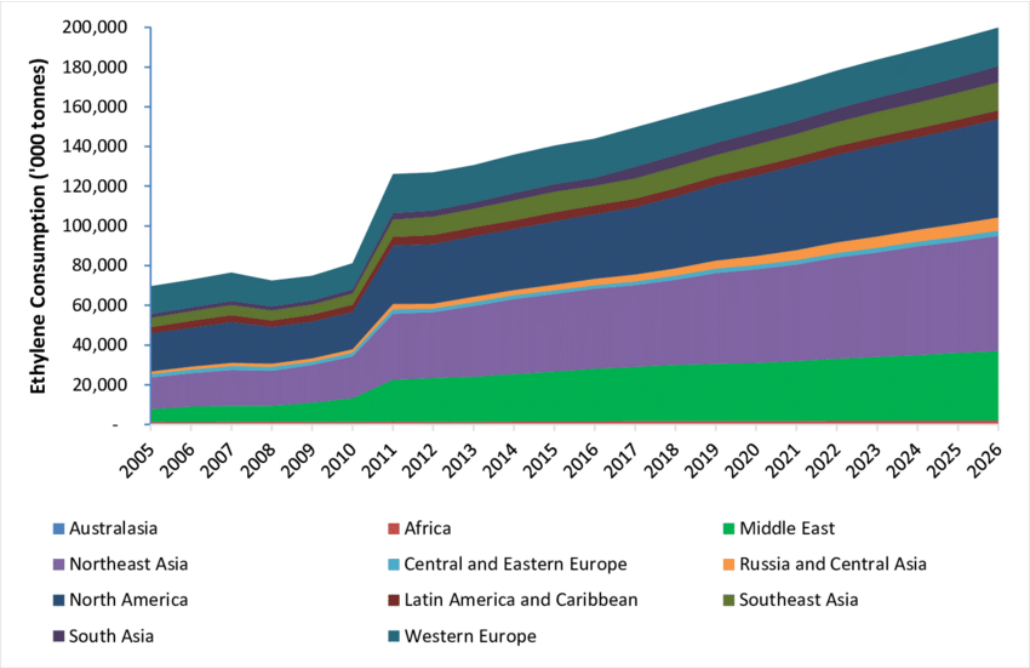

Figure 2.3: Global ethylene demand by geographic area [1].

2.1.2 Bioethanol

At the moment, bioethanol is considered as one of the main alternatives for the production of ethylene [10]. The process of producing bioethanol from biomass sources is fairly simple since it only includes a fermentation step. On top of this, ethanol produced from biomass is chemically similar to the one obtained synthetically from petroleum. There are four different categories of biomass that can be used: sugar-based biomass, starch-based biomass, lignocellulose-based biomass and lastly marine species, which is a very promising route once land becomes scarce [11].

The first constitutes the main feedstock for the so-called first-generation fermentation for bioethanol production, which thus processes feedstock with a high level of sugar or starch and is the most commonly used method of production. However, there are different opinions among people because it is claimed that it consumes crops that could be allocated as human or animal food [12].

Lignocellulosic and marine biomass are considered second-generation feedstocks. The second generation technology is still in the need of more developments but already has some advantages especially the fact that it does not use food crops. Instead, it uses agricultural residue, which has high availability and can be found for much lower prices [13].

Feedstock to be used for bioethanol production often depends on the part of the world where it is and climatic conditions. For example, in Europe sugarcane is more used in contrast to the USA where starch-based crops are preferred [14].

In 2011, the global ethanol production was already over 100 billion litres with a yearly increase of 3 to 7% over the past decade [13]. Furthermore, around 80% of total world ethanol production, already comes from biomass fermentation, with Brazil and the United States of America being the main contributors to it, representing a share of around 31% and 42% each, respectively. Alongside this, reports claim that from 2016 until the year 2024, a rise of 34% will be observed in ethanol production [15, 16].

Even though these numbers might seem promising, the economics of the process of ethanol dehydration to ethylene when the ethanol has biomass as its source, are still not competitive with the more common production technologies. The main reason is the high price of the bioethanol, making either ethylene quite expensive or the production not very profitable [7]. So prospects say that these alternative resources and technologies will work together with steam cracking technology, which is the most common one, instead of replacing it. Leading to the creation of more sustainable processes, while having still good results in terms of conversion and operating conditions [2, 17].

2.2 Ethylene production technologies

2.2.1 Conventional technology-Steam cracking

Steam cracking is a well-established technology, developed in the 1960s, that is considered to be the current leading technology for the production of ethylene and other olefins, like propylene, for example [2]. It consists of a petrochemical process that breaks down saturated hydrocarbons into smaller molecules. For that, a gaseous or liquid hydrocarbon input, such as naphtha, Low Pressure Gas (LPG), or ethane, is diluted with steam and heated in a furnace in the absence of oxygen [5, 6]. A brief flow diagram for the process is presented in Figure 2.4 when the used feedstock is natural gas [6].

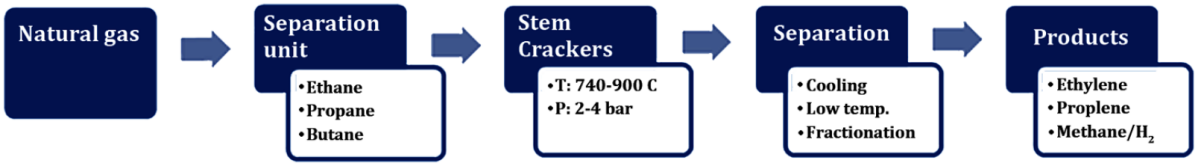

Figure 2.4: Flow Diagram for ethylene production through steam cracking [6].

Firstly, natural gas passes through a separation unit where different types of hydrocarbons, like ethane or propane, are separated. This mixture of ethane, propane and other hydrocarbons goes further to a steam cracker where cracking reactions happen forming a fraction of lighter hydrocarbons. Steam cracker effluent goes then to a second separation unit to be quenched to temperatures around 600 °C, being cooled down after in a subsequent stage to around 300°C. This sequential cooling has the

objective of preventing degradation by secondary reactions and also generating steam for the compressors, promoting energy integration among the process. The reaction temperature is high, normally in the range of 850°C with low residence times, which leads to very high gas velocities. The hydrocarbon to steam ratio can also heavily influence the outcome of the process [6, 18].

Even though being a very well-established technique, with some improvements and developments over time, steam cracking still has many drawbacks attached to it. The first one is related to the higher temperatures at which the process occurs, implying higher operational costs. Secondly, there is a tendency for secondary undesired reactions to occur. Additionally, deactivation of the catalyst by coke deposition happens quite often during the process [5]. Apart from the operational challenges, there are several environmental issues with this process, mainly with CO_2 emissions. It is reported that steam cracking processes account for around 300 tons of CO_2 emissions annually and some years ago it represented around 30% of the total emissions associated with the chemical industry [19, 20].

2.2.2 Alternative technologies for ethanol production

2.2.2.A Catalytic dehydration of ethanol to ethylene

Catalytic dehydration of ethanol into ethylene appears as one of the main alternatives for ethylene's main production process. It is a process that has been known for a long time but has never been exploited for large-scale ethylene synthesis, mainly due to the operational cost and raw material availability [5, 21]. However, with the increasing production of bioethanol, this process becomes a better perspective. Not only this could solve the environmental problems related to the conventional steam cracking route, as it would lead to a disruption of ethylene's value chain reliance on crude oil price fluctuations [5].

Industrially, the process can be divided into three different parts. The first one contains the reactional part where the dehydration occurs, the second one includes the recovery of ethylene and the third consist of its purification. As presented in Figure 2.5, preheated feedstocks flow into a reactor where an endothermic reaction takes place, forming ethylene, which afterwards goes into washing towers and dryers where byproducts like diethyl ether, for example, are separated [8].

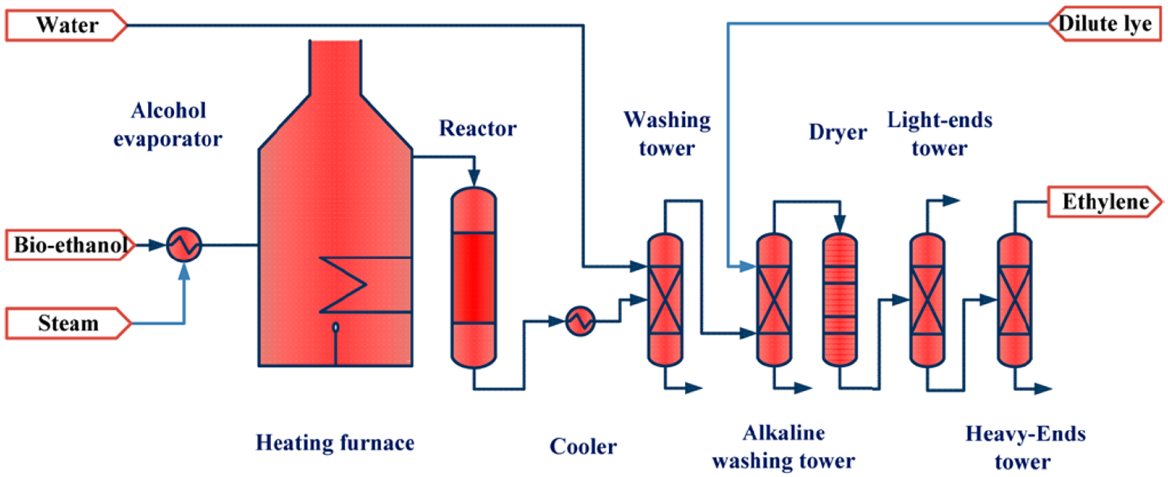

Figure 2.5: Process diagram for an ethylene production plan [8].

The operating temperature in the reactor unit depends on the wanted fraction of each product. Namely at the temperature above 473 K, ethylene is the main product, while below this temperature, it is the ether [22].

The reactor used can either be a fixed bed or a fluidized bed reactor. At the moment, the fixed bed is the most used in industry. A usual configuration is a multitubular disposition with the catalyst placed inside the tubes and a hot fluid passing outside on the shell [23]. The conversion obtained with this kind of reactor is around 99% with a selectivity of 95% to 99% when using zeolites like HZSM-5 or ZSM-5, for example [3, 24]. Scaling-up of the reactor is limited due to the difficulty in maintaining an uniform temperature along the tubes when they become bigger [10].

A fluidized bed reactor is a very promising alternative. When compared to the fixed bed reactor, this one, has similar behaviour in terms of results while having less catalyst deactivation due to coke deposition and having less operational costs associated because it does not need an external source of heat. But it still has some problems to be solved, mainly related to collision between the catalyst particles and the reactor walls, which could cause damage to the catalyst [8].

In the recovery step, the water, carbon dioxide and ethanol that did not react are set to be removed. The water is firstly removed, by using a quenching tower. The carbon dioxide is removed by dissolution in a sodium hydroxide solution and then the remaining water is removed by molecular sieves. It is very important to remove this water because the instruments to be used in the purification phase are very sensitive to the water content of the stream. Lastly, the purification step consists of a cryogenic distillation unit that removes all the impurities from previously cooled ethylene. In the end, the obtained ethylene normally has a purity level of around 98% [10].

This process has some downsides. At the moment, the price of ethanol as a feedstock determines the cost of ethylene synthesis and the price of pure ethanol is still quite high. On top of that, the price

of the produced ethylene following this route is not comparable to the one produced by steam cracking. This issue can be, at least partially, tackled if bioethanol is used as a feedstock. Another solution for this problem can be the usage of ethanol with lower purity levels, but this hypothesis still needs more studies and research before implementation, since the effect of the impurities in the process needs to be studied and simulated, to assess its feasibility [10].

Catalysts

Ethanol dehydration can be considered as an acid-catalyzed reaction. Many different catalysts have been studied so far, to achieve maximum selectivity and conversion. Those include transition state metal oxides, alumina, zeolites, etc [25].

A – Phosphoric acid catalyst

The first used catalyst for the studied reaction was a catalyst of phosphoric acid. The *British Imperial Chemical* created it in the 1930s by depositing phosphate on coke or clay. In fact, until the 1950s, this catalyst was the base one for the production of polyethylene in England [25]. This, at the time, presented a product with high purity but, on the other hand, the catalyst suffered quick deactivation due to the deposition of coke. As the catalyst required a month to regenerate, the use of this catalyst was abandoned [25].

B – Alumina-based catalyst

In the years that came after this, alumina-based catalysts were utilized. They were first used in Germany by a company called *Elektrochemische Werke*. Many have followed the same path, like *Braskem* in Brazil which produced ethylene as a raw material for the production of polyethylene and other polymers [7, 25].

The alumina-based catalyst exhibited better results than the previous one in terms of ethylene purity. However, for it to work properly, the ethanol concentration at the beginning of the process needs to be higher, otherwise higher temperatures and lower space velocities will be required, leading to higher energy-related expenses, thus making the process unfeasible. Because of this many companies ended up their ethylene production through this process and turned again to the steam cracking path [8, 25].

C – Heteropolyacid catalysts

Heteropolyacid refers to an oxygen-containing multi-acid created by the core atom that can be P, Si or Fe, for example, and the ligand-atom which can be Mo, V, W, bridging the oxygen atom, as can be seen in Figure 2.6 [8].

Due to their physicochemical properties, heteropolyacid catalysts are considered a promising family of catalysts both for heterogeneous and homogeneous catalysis. They are also considered to be useful as a model system, being very used for fundamental research, to explore some problems that still exist in catalysis because their acidity and oxidizing potential can be easily modified [26].

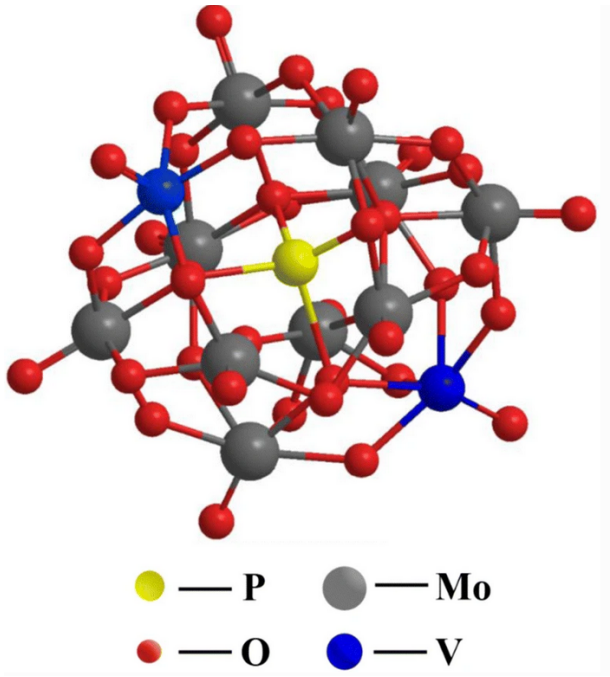

Figure 2.6: Structure for one of the main variants of a heteropolyacid catalyst [27].

The use of this type of material for ethanol dehydration to ethylene offers several advantages including lower reaction temperatures with higher conversion rates. Yet, this type of catalyst needs to be loaded on the carrier when utilized, which results in higher preparation costs and can lead to big losses. As a result, even though this catalyst can be a promising one, as stated before, more research into it is still required [8].

D – Zeolite catalysed reaction

Lastly, the type of catalyst that has been studied and utilized more recently is zeolites. Zeolites are promising materials as catalysts due to their unique structural properties, especially their big internal surface area which can lead to a higher number of active sites available for reactions. As reported by Tanabe *et al.* [28], almost 40% of the industrial processes are already improved by the use of zeolites as catalysts.

There are zeolites originating from nature, but these are considered unsuitable due to their high water content and the presence of impurities. Since the 1970s, big efforts have been made to develop synthetic zeolites, especially to catalyze reactions in the petrochemical area. In 1972 Mobil managed to

synthesize the first zeolite, with a main focus on improving petrochemical processes [25].

A zeolite is an inorganic molecule made up of tetrahedron of SiO_4 and AlO_4 linked by a common oxygen atom, with the following general formula given by Equation (2.1), where A represents the anion, x/y the ratio of silica atoms over aluminium and (x+y) the amount of tetrahedron per unit cell [25].

$$A^{m+}_{y/m}[(SiO_2)_x.(AlO^-_2)_y].zH_2O \tag{2.1}$$

This link between the tetrahedrons results in a porous molecule with a 3D structure, as can be seen in Figure 2.7, where four of the main zeolite structures are presented [29].

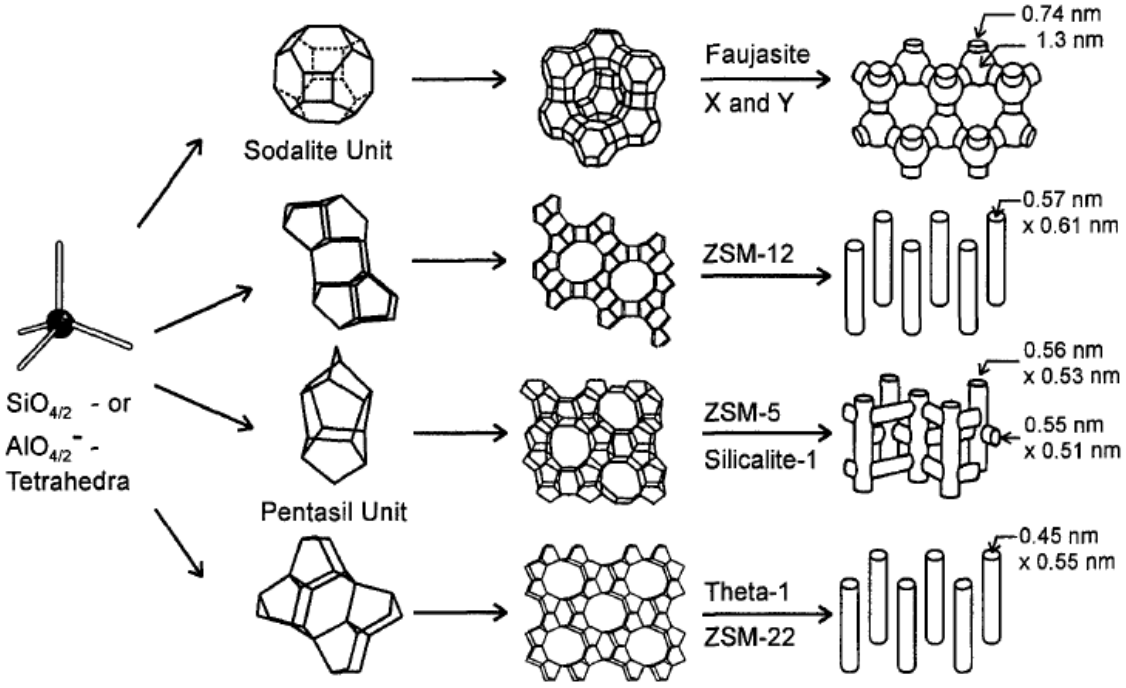

Figure 2.7: Structure of four of the main zeolites. [29].

Three important characteristics that are present in zeolites are shape selectivity, the confinement effect and the Si/Al ratio. These characteristics can be manipulated to optimize the reaction results.

Shape selectivity, as the name says, means that the transformation of reactants depends on how the molecules fit in the pores/channels of the zeolite. It is based on the idea that the pores of some zeolites are of the same order of magnitude as the reactant molecules in terms of molecular dimensions. This will cause some molecules to not adsorb and certain possible reaction products might not be formed. This is a very useful characteristic for diminishing the production of undesired by-products in some reactions [30, 31].

The confinement effect consists of a property related to the porous structure, that is known to have a high influence on the diffusion step. This leads to a constrained environment due to geometrical

constraints and selective absorption affecting the reactions selectivity and activity [32].

Last but not least, the Si/Al ratio is also a characteristic with a very high influence on catalyst performance since it defines the Brønsted acidity of the catalyst when the cation is exchanged for a proton. Reports claim that, when the ratio is low, so when alumina is present in higher concentrations, the acid site density will be higher. But, the presence of more acid sites means more AlO_4-tetrahedron leading to a decrease in the acid site strength, even though they are present in bigger quantities [25]. Finding a balance between these relationships is the key element that should be adjusted according to the objective of each process.

Lewis acid sites are another type of acid site that can be present on zeolite surfaces. These can be formed from non-framework aluminium species which can appear by degradation of Brønsted acid sites along with some thermal treatment. They are of much less importance and exist in lower concentrations than Brønsted acid sites [29].

Zeolites show higher activity than alumina-based catalysts allowing for lower reaction temperatures however they can be more prone to deactivation [25].

Considering this, looking for new approaches for catalyst development, which is one of the aims of this paper, remains very important.

In recent years, catalyst modification has been often implemented to improve their performances and lifetime. These modifications are heavily important in establishing relationships between catalyst properties and performances. The most common ones are related to dealumination processes and metal doping. The major objective in performing these modifications is to reduce the number of strong acid sites on zeolite structure as it has been realized that the weak acid sites have a bigger lifespan regarding coke deposition and provide better catalyst stability [3].

Dealumination can be classified as a demetallation post-synthesis method that has the aim to remove aluminium from the catalyst structure by utilizing hydrothermal treatments or other chemical agents.

Not only this method can cause changes in the number of acid sites of the zeolite but it also breaks down its structure, leading to the formation of vacant spots. This can further increase the porosity, especially regarding mesopores [33].

Similar to dealumination there is another demetallation process called desilication. It is one of the most used processes to create secondary porosity in zeolites structure. This technique removes silicon from the zeolite structure preferentially in an alkaline environment. In the resulting material, microporous nature and acidic characteristics are preserved and a secondary system of mesopores is formed, which impacts the activity, selectivity and lifespan of the material [33]. Catalysts obtained by this technique can be considered hierarchical catalysts since they possess the inherent catalytic characteristics of microporous zeolites but with improved access to and transport through the extra meso and macroporous system that the material retains [34]. Figure 2.8 demonstrates a simple chemistry of the hydrolysis

process that results in either dealuminated or dessilicated zeolites.

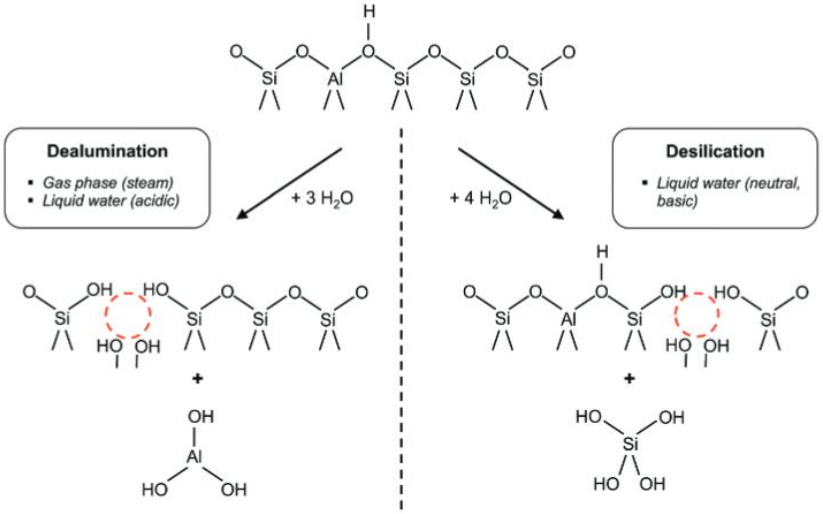

Figure 2.8: Hydrolysis processes involved in the synthesis of dealuminated and dessilicated zeolites [35].

Metal doping is a post-synthesis process that consists of two main steps. Firstly, a proton substitutes a cation in the zeolite followed by metal impregnation on the zeolite [36]. This cation insertion followed up by the ion exchange can induce the change of the zeolite physical properties for example the crystallinity or the porous structure [37].

In the particular case of doping with phosphorous, it is reported that this kind of doping will improve shape selectivity through a replacement of the stronger acid sites and also diminish the pore size, which can strongly influence the diffusion of components inside zeolite structures [38].

Mechanism

Regarding the reaction mechanism for the zeolite catalyzed ethanol dehydration to ethylene, it is quite consensual among many studies [22, 39]. It is suggested that the reaction happens via two different competitive paths as demonstrated in Figure 2.9. The first one (path A in Figure 2.9) is an ethanol dehydration to water and ethylene and is thermodynamically endothermic, while the second (path B) is an exothermic bi-molecular step where ethanol is dehydrated into water and diethyl ether. There is also a third path (path C), that embodies a diethyl ether conversion to ethylene and ethanol. The dominant product at lower temperatures (323-373K) is ether, while at higher temperatures (373-473K) ethylene becomes the major product. The reaction temperature is a major variable in the process that needs to be controlled, since undesired reactions, such as, oligomerization reactions start occurring at higher temperatures, leading to the formation of higher hydrocarbons [22, 40].

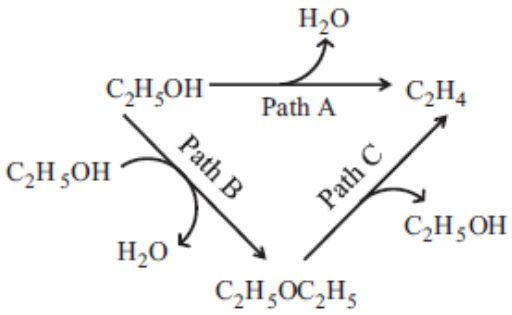

Figure 2.9: Reaction scheme for ethanol dehydration reaction [11].

Figure 2.10, shows the proposed mechanism of ethanol dehydration to ethylene. This mechanism was obtained through Density Functional Theory calculations and was validated by several kinetic experiments. In Table 2.1, the three paths mentioned above (shown in Figure 2.9) are presented, with their contribution for each one of the paths.

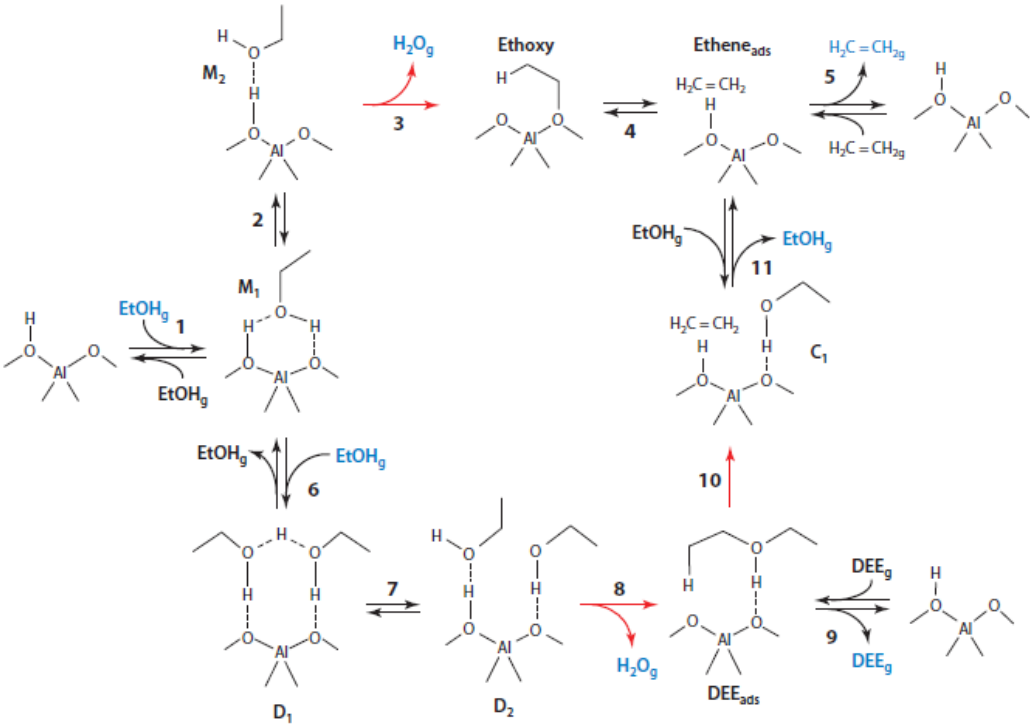

Figure 2.10: Reaction mechanism for the dehydration of ethanol to ethylene [22].

Table 2.1: Reaction Mechanism and Steps [22].

Step	Elementary Step	A	B	C
1	$C_2H_5OH + * \leftrightarrow M1$	1	1	0
2	$M1 \leftrightarrow M2$	1	0	0
3	$M2 \leftrightarrow Ethoxy + H_2O(g)$	1	0	0
4	$Ethoxy \leftrightarrow Ethene_{ads}$	1	0	0
5	$Ethene_{ads} \leftrightarrow Ethene(g) + *$	1	0	1
6	$M1 + C_2H_5OH \leftrightarrow D1$	0	1	0
7	$D1 \leftrightarrow D2$	0	1	0
8	$D2 \leftrightarrow DEE_{ads} + H_2O(g)$	0	1	0
9	$DEE_{ads} \leftrightarrow DEE(g) + *$	0	1	-1
10	$DEE_{ads} \leftrightarrow C1$	0	0	1
11	$C1 \leftrightarrow Ethene_{ads} + C_2H_5OH$	0	0	1
Path A	$C_2H_5OH(g) \longrightarrow Ethene(g) + H_2O(g)$			
Path B	$2C_2H_5OH(g) \longrightarrow DEE(g) + H_2O(g)$			
Path C	$DEE(g) \longrightarrow Ethene(g) + C_2H_5OH(g)$			

Starting with path A, it is a monomolecular pathway which includes ethanol adsorption, forming a chemisorbed monomer named M1 (adsorbed ethanol). Species M1 undergoes a rearrangement forming physisorbed surface species M2. After that, M2 undergoes water elimination due to activation of the alcohol C_α-O bond. This activation occurs by the catalyst proton promoting an attack of the α carbon by the aluminun-bound oxygen next to the acid site, leading firstly to the formation of a cationic transition state followed by the formation of an ethoxide. From this, physisorbed ethylene is formed, desorbing after with regeneration of active sites [22].

With path B, not only one but two ethanol molecules adsorb forming D1, which is a chemisorbed dimer, where both of the molecules that adsorbed share the proton. Similarly to what happens in path A, this intermediary species undergoes a rearrangement, forming physisorbed D2. This step is necessary for the elimination of water, leading to the formation of the Diethyl Ether (DEE) species. This one then desorbs which frees the active sites [22].

Considering Path C, an attack of the β-hydrogen of a previously adsorbed DEE molecule by the aluminum-bound oxygen next to the acid site leads to the scission of the C_β-H and C_α-O bonds forming physisorbed ethylene and ethanol. Following this, both these compounds desorb restoring acid sites [22].

K. Alexopoulos et al. proposed a mechanism based on Density Functional Theory (DFT) calculations, which is somewhat a more complex one, as shown in Figure 2.11 [39]. The kinetic model for this study was developed around this adopted mechanism and MDCD was performed considering it because this model has already been used for kinetic modelling and is reported to be a valid one for the process [39]. Furthermore, it was chosen instead of the more simplistic one, presented previously, to have a more accurate study of the behaviour of the process. This mechanism accounts for the same three reaction paths as the previous one shown in Figure 2.10 but comprises eight different mechanisms among those

paths. Path A consists of five mechanisms, path B consists of two mechanisms and path C is just one shown in Table 2.2.

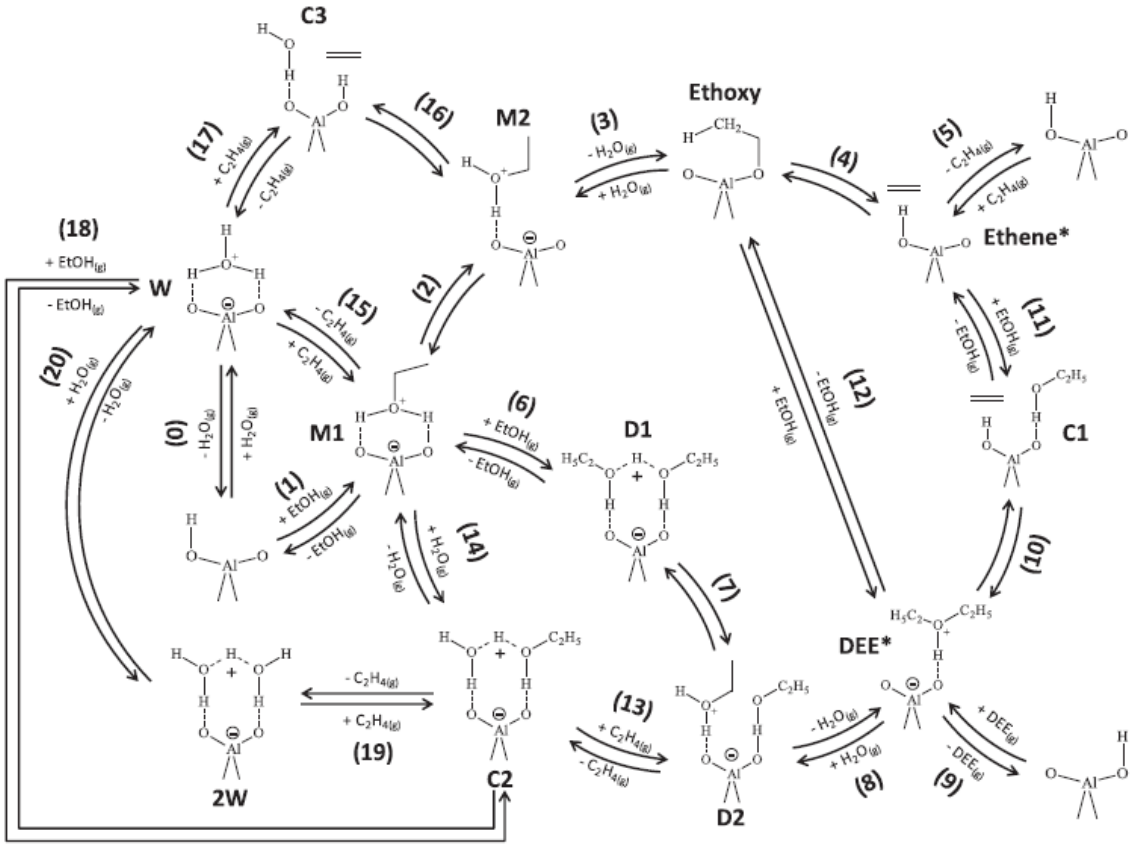

Figure 2.11: Complex reaction mechanism for the dehydration of ethanol to ethylene [39].

For path A, one of the mechanisms assumes that the ethylene formation can happen in the following way. Firstly (step 1), adsorption and protonation of ethanol take place forming intermediate M1, followed by elimination and desorption of ethene as stated by step 15, with deprotonation of water (step 0). M1 goes through heterolysis of the C-O bond led by deprotonation of the β-carbon forming the ethylene. The second mechanism that *K.Alexopoulos et al.* proposes is the same as the one proposed in Table 2.1 for path A [39]. A third mechanism is constituted by, firstly, the ethanol protonation and adsorption in step 1, followed by a rearrangement of the surface species formed in 1 (step 2), followed by elimination of ethene (step 16), with its consequent desorption (step 17). Lastly, there is, of course, the de-protonation and desorption of water (step 0). The fourth mechanism is a path that was recently discovered and claims that water is needed together with ethanol since it assumes that the process occurs on an acid site previously covered with water. Following this assumption, the first step consists of ethanol adsorption together with water (step 18), followed by ethylene desorption and elimination. After this, water desorbs from the formed dimer (step 20) [39]. The last mechanism presented for path A is a simple one, where

instead of having a pre-adsorbed water molecule as it happens in the previously explained mechanism, there is the need to have an adsorbed ethanol molecule. This starts with ethanol adsorption on the ethanol monomer that is already protonated (step 6), followed by a rearrangement of the formed dimer (step 7), and then elimination and desorption of ethylene (step 13), The last step of this mechanism consists on the desorption of water from the formed intermediate (step 14) [39].

For path B, one of the proposed mechanisms is the same as path B of the simpler mechanism (shown in Figure 2.10), being an ethoxy-mediated one. The second proposed mechanism includes a dimer-mediated process. It starts with monomolecular adsorption of ethanol (step 1), followed by bi-molecular adsorption of ethanol (step 6), forming the species D1. Then a rearrangement of the dimer happens, producing the intermediate D2 (step 7). After that, a protonated ether is formed by a nucleophilic substitution (step 8) and lastly, DEE desorbs and de-protonates, freeing the acid active site [39]. In step 8 the C_α of the protonated ethanol destroys its bond with the water group and bonds with the oxygen of the ethanol molecule [39].

Regarding path C, the proposed mechanism is equivalent to the one from the first proposed mechanism, with almost no differences between them [39].

Table 2.2: Elementary steps and reaction mechanisms for ethanol dehydration in H-ZSM5 [39].

	Path #	A				B			C
	Mechanism #	**1**	**2**	**3**	**4**	**5**	**6**	**7**	**8**
(0)	$W \leftrightarrow H_2O(g) + *$	1	0	1	0	0	0	0	0
(1)	$EtOH(g) + * \leftrightarrow M1$	1	1	1	0	0	1	1	0
(2)	$M1 \leftrightarrow M2$	0	1	1	0	0	1	0	0
(3)	$M2 \leftrightarrow ethoxy + H_2O(g)$	0	1	0	0	0	1	0	0
(4)	$Ethoxy \leftrightarrow Ethene*$	0	1	0	0	0	0	0	0
(5)	$Ethene* \leftrightarrow C_2H_4(g) + *$	0	1	0	0	0	0	0	1
(6)	$M1 + EtOH(g) \leftrightarrow D1$	0	0	0	0	1	0	1	0
(7)	$D1 \leftrightarrow D2$	0	0	0	0	1	0	1	0
(8)	$D2 \leftrightarrow DEE * + H_2O(g)$	0	0	0	0	0	0	1	0
(9)	$DEE* \leftrightarrow DEE(g) + *$	0	0	0	0	0	1	1	-1
(10)	$DEE* \leftrightarrow C1$	0	0	0	0	0	0	0	1
(11)	$C1 \leftrightarrow Ethene * + EtOH(g)$	0	0	0	0	0	0	0	1
(12)	$Ethoxy + EtOH(g) \leftrightarrow DEE*$	0	0	0	0	0	1	0	0
(13)	$D2 \leftrightarrow C2 + C_2H_4(g)$	0	0	0	0	1	0	0	0
(14)	$C2 \leftrightarrow M1 + H_2O(g)$	0	0	0	0	1	0	0	0
(15)	$M1 \leftrightarrow W + C_2H_4(g)$	1	0	0	0	0	0	0	0
(16)	$M2 \leftrightarrow C3$	0	0	1	0	0	0	0	0
(17)	$C3 \leftrightarrow W + C_2H_4(g)$	0	0	1	0	0	0	0	0
(18)	$W + EtOH(g) \leftrightarrow C2$	0	0	0	1	0	0	0	0
(19)	$C2 \leftrightarrow 2\,W + C_2H_4(g)$	0	0	0	1	0	0	0	0
(20)	$2\,W \leftrightarrow W + H_2O(g)$	0	0	0	1	0	0	0	0
Path A	**(mechanism # 1-5)**	$C_2H_5OH(g) \longrightarrow Ethene(g) + H_2O(g)$							
Path B	**(mechanism # 6-7)**	$2C_2H_5OH(g) \longrightarrow DEE(g) + H_2O(g)$							
Path C	**(mechanism # 8)**	$DEE(g) \longrightarrow Ethene(g) + C_2H_5OH(g)$							

2.2.2.B Other alternative technologies for ethanol production

Alongside the ethanol dehydration into ethylene technology, there are more emerging technologies for ethylene production, that can compete between them to be the main production technology in the future. This is driven by the existence of cheap alternative feedstocks to naphtha such as propane, ethane or methane, especially in the United States of America, where the production of shale gas has risen exponentially. Moreover, since methane is very abundant and can have a lower price, all technologies that have the ability to transform it into higher hydrocarbons or chemicals with high value are considered to be very promising and a good studying topic [2]. Anyhow, for these technologies to be able to come into play at a bigger scale, they need to economically match the current steam cracker plant and production capacity. So development needs to be done regarding capital costs, process efficiencies and reliability so the risk of investing in these is as low as possible.

Nonetheless, some of the processes from these groups are considered promising. These are the MtO, the FTS, the OCM and the Oxidative dehydrogenation of light alkanes (ODH) as can be seen in Figure 2.12 [2].

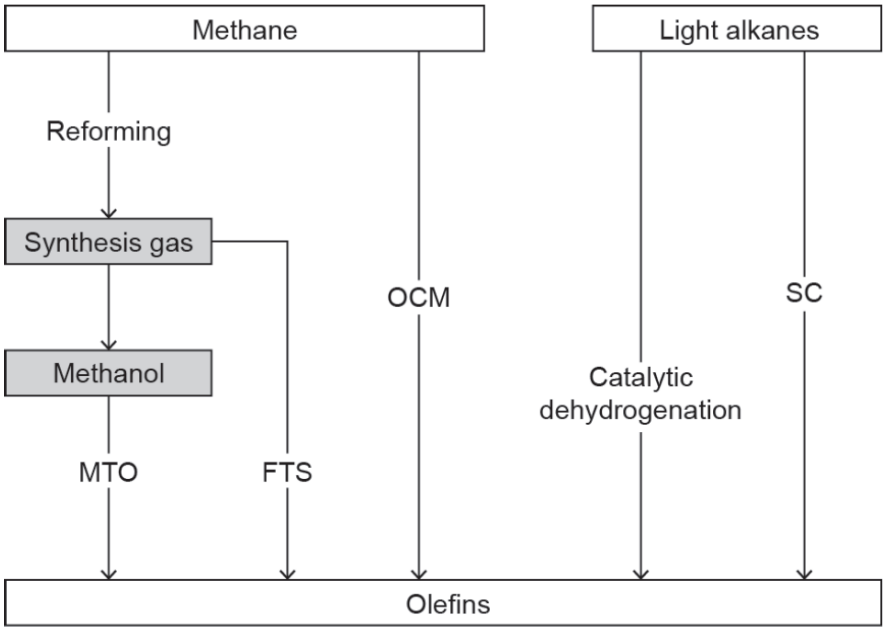

Figure 2.12: Different technologies for ethylene and other olefins production [2].

A – Methanol to olefins

The MtO process was developed by Mobil in 1977 and further patented and developed by other companies like UOP/Hydro, for example. It is a process where methanol, previously obtained from natural gas or coal, is catalytically dehydrated and then converted into ethylene over zeolite or alumina

catalysts [41]. In the case of Mobil's process, ZSM-5 is used, while silico-alumino phosphate (SAPO-34) is used at UOP/Hydro [2]. The MtO process is carried out in a fluidized bed reactor with a yield of around 80% in terms of carbon content.

At the moment China is the country boosting this technology the most, mainly due to governmental policies since it has large quantities of coal to use as raw material. Proving this is the capacity of production of olefins from coal that has increased from 1.1 million tons per year to 15.5 million tons per year [2].

The process seems to be economically competitive with the conventional method but still needs a lot more research and upgrades to deal with catalyst deactivation, mainly caused by coke deposition, and regeneration.

B – Fischer-Tropsch synthesis

Regarding the FTS process, this is a mature catalytic process that aims at the production of liquid fuels and other chemicals, like linear alkanes, alkenes and oxygenates from syngas, which is a mixture of CO and H_2, normally obtained from the reforming or gasification of methane. It is seen as a very beneficial process, especially in areas where the amount of crude oil is meagre [2].

For FTS to be a process for olefin production, some problems still need solving. These problems are very catalyst dependent and involve a lack of control on the reaction's product selectivity, leading to a very broad range of products, and sulfur poisoning [42]. Furthermore, from already implemented industrial units, the investment and risk associated with FTS units can be much higher than expected initially [2].

C – Oxidative coupling of methane

The OCM process is a direct conversion route of methane to other hydrocarbons by activating methane to produce methyl radicals [2]. These methyl radicals can combine to originate ethane, that by going through a set of pyrolysis reactions can form ethylene. Similarly to the ethanol dehydration to ethylene, this technology does not need crude oil as a raw feed, making it one of the most researched ones, so it can be commercialized in a few years.

If methane is available abundantly and at low prices, this technology can be feasible and very competitive [17]. However, research in terms of catalyst design to enhance the selectivity and stability at higher temperatures is still required. Additionally, the development of new reactor technologies is needed to deal with the high exothermicity of the reaction and make thermal control easier [2].

D – Catalytic dehydrogenation of light alkanes

Another emerging technology for olefin production is the ODH. Due to the high quantity of cheap light alkanes, that can be produced from shale gas, it is worth considering this process. Especially in

countries like China that is reported to have shale gas reserves of up to 207 trillion cubic meters or the United States where the projections claim that almost 50% of the natural gas produced by 2040 will come directly from shale, according to the Energy Information Agency (EIA) [43].

At the moment there are already two patented processes for this technology, Oleflex and Catofin. The reactions for this transformation are heavily endothermic, being favoured at high temperatures and lower pressures over alumina-supported catalysts [2].

The biggest downside of ODH at the moment is a tendency for coke formation and deposition on the catalyst which is pronounced at the temperatures required for a higher ethylene selectivity. Coke formation is not fully reversible, which, of course, compromises the catalyst activity and lifetime, therefore, further research in the area of catalyst stabilization and recovery is needed [2].

On top of this, the energy efficiency of the process still needs to be improved, as well as the reaction equilibrium that should be shifted to the product side. For that, some strategies are being tested like lowering the partial pressure or removing hydrogen from the system. However, problems associated with thermal stability arise and still need solving [2].

Environmental concerns

The main reason for these processes to be considered promising, as stated before, is environmentally related.

The ethanol dehydration to ethylene technology solves a big part of the issues related to steam cracking. Firstly, since it needs very lower temperatures to work, the energy consumption by the ethanol dehydration to ethylene is much lower, having lower operational costs associated with it. Secondly, the CO_2 emissions per ton of ethylene produced are reported to be around 60% lower than the ones from steam cracking, when the process gets more developed. On top of that, this process, if the raw material is bioethanol, can be considered almost carbon-neutral, because the CO_2 released into the atmosphere during the combustion of ethanol, was previously absorbed by the growth of crops and other biomass sources during the process of photosynthesis. The emissions of NO_X and other particulate matter are also much lower for this process [5].

Figure 2.13 shows the total emissions of CO_2 coming from various routes for ethylene and other olefins productions. A distinction between two kinds of CO_2 is made. One is energy-related CO_2 , for example, produced by the fuel combustion or power generation needed to heat the process to the required temperatures, and the chemical CO_2 that is produced in the reaction [2].

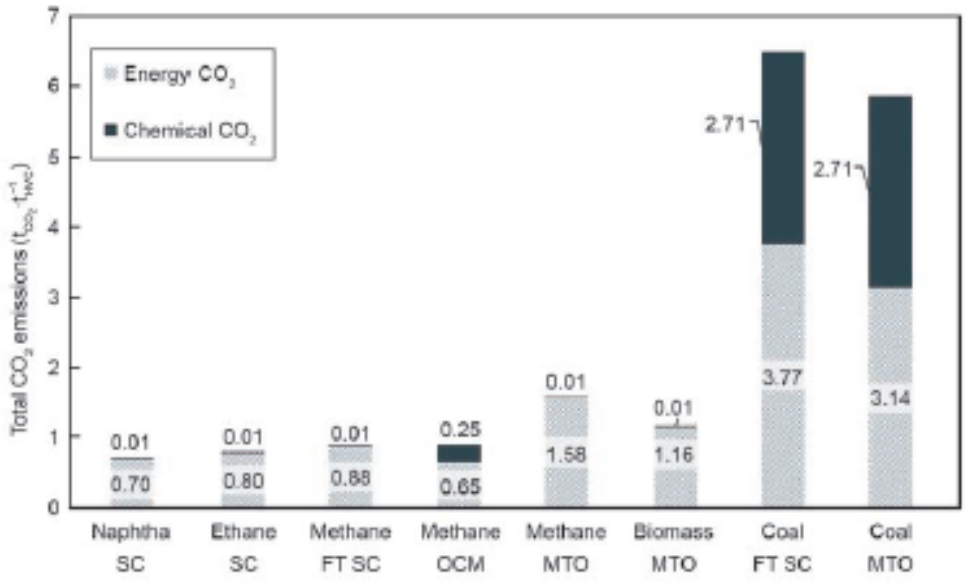

Figure 2.13: Total CO_2 emissions per ton of chemicals for different production technologies [2].

It is clear from the figure that SC, when using naphtha or ethane as feedstock, is still the best technology mainly because of all the development and research put into it, which lead to the high energy efficiency of the process. However, if big efforts are done on the alternative processes presented, these can become similar or even better than SC. OCM, for example, already showed very good results, which can be easily further reduced in terms of chemical CO_2 if the selectivity for ethylene in the process is improved [2].

2.3 Catalyst development techniques

Catalysis and catalysts are present in all forms of chemicals in the industry. It is commonly said that at least one catalytic process is used in the manufacturing of over 90 % of all chemical products [44]. So it should come as no surprise the fact that the search for novel catalytic materials is a never-ending process. This aspect in chemical industry became even more important with the development of new sustainable ways to manufacture chemicals relying less on fossil fuels [45, 46]. However, designing a catalyst is a difficult task, mainly due to the complexity of solid materials and heterogeneous catalysis, which requires an understanding of multiple scientific fields, from surface science to chemical reaction engineering.

Since the beginning of the research, catalyst development has frequently depended on ”trial and error” techniques, where laboratory-size performances are assumed to be representative of industrial-scale operation. Despite numerous attempts to rationalize the development of new catalytic materials, by trying new approaches and techniques, the ”chemical experiment” keeps being a very credible tool for

new catalyst development, giving information about several important parameters like conversion, selectivity, stability... Nevertheless, with the introduction of high-throughput testing, the number of experiments that need to be done in a laboratory became less limiting, being the interpretation and management of obtained data the main restriction now [4]. The main improvements of this approach are situated around using statistical techniques such as Design of Experiments (DoE), for example. DoE technique is a statistical method for optimizing a specific response by taking into account the various factors that contribute to the output. For example, in chemical engineering, this can be used to optimize the yield of a specific reaction taking into account temperature or pressure as the process variables. This approach gives the ability to explore the whole factor space and determine relevant combinations of factors to optimize the objective function [4, 47].

In terms of catalyst design techniques, there are three main ones:

- Statistics-Driven Catalyst Design
- Performance-Driven Catalyst Design
- Information-Driven Catalyst Design

Statistics-Driven Catalyst Design

In this catalyst design approach, catalyst properties that have to be optimized as well as the interval where they will be modified need to be selected. This optimization is then performed by using an "one-variable-at-a-time" principle. As the name says, this consists of a method where the design of experiments involves the testing of one variable at a time to be able to investigate its effect on the product quality and quantity [4, 47]. Instead of applying this principle, more sophisticated statistical methods can also be used. A full factorial design is an example of this statistical methods, that can be used over a big range of experimental conditions. However, the number of experiments, that would need to be performed, when using this method, would be enormous and very time-consuming. A design type that could solve this problem is a fractional factorial design. For this kind of method, a correlation is made between the catalyst characteristics(x_i) and its performance(y). This presents a linear behaviour for the parameters (b_1) and a quadratic one for interaction terms, as can be seen in Equation (2.2) [4].

$$y = b_0 + b_1 x_1 + b_2 x_2 + b_3 x_1^2 + b_4 x_2^2 + b_5 x_1 x_2 \tag{2.2}$$

Although this technique may have good outputs in terms of catalyst design and performance assessment, it has some drawbacks. The main one is the fact that the relations like the one from Equation (2.2), have a deficiency in terms of the fundamental detail that governs the catalyst performance. This makes this kind of relation more adequate for interpolations but very poor in what extrapolations are concerned.

Accordingly, it can be considered as an insignificant method for studying how the catalyst works and reacts to different operating conditions, like temperature, pressure or other feedstocks [4].

As a consequence, the choice of catalyst might not be optimal.

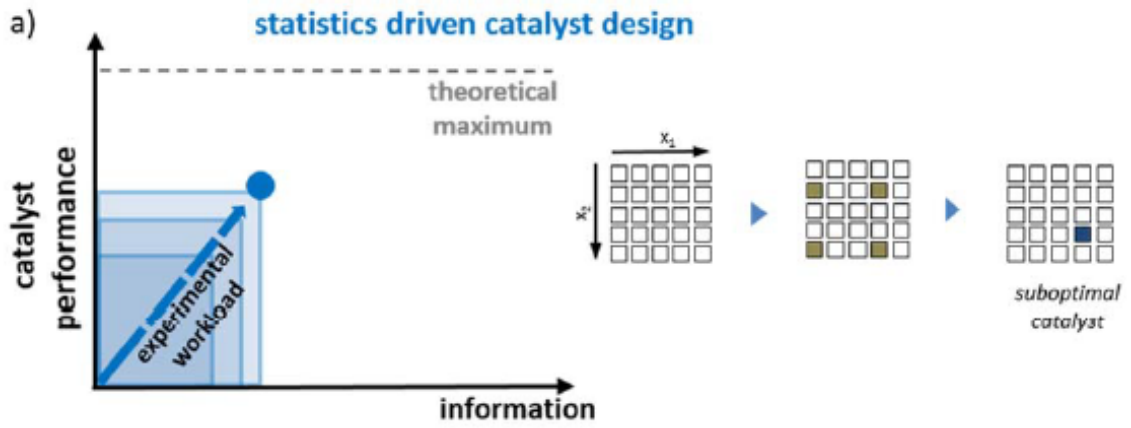

Figure 2.14: Statistics-Driven design methodology [4].

Performance-Driven Catalyst Design

The Performance-driven catalyst design technique is the most intensive method. In contrast to the method presented previously, this methodology generally differentiates between two stages. One consists of a catalyst screening stage and the other of an optimization stage.

In the first one, a big amount of catalysts are prepared, studied kinetically and ranked based on their performance. In the second stage, the catalyst that, previously, had interesting results are tested more thoroughly, to find the better one. This technique has a big drawback because it needs the synthesis and testing of a large amount of materials, which can take up a lot of time and money [4, 25].

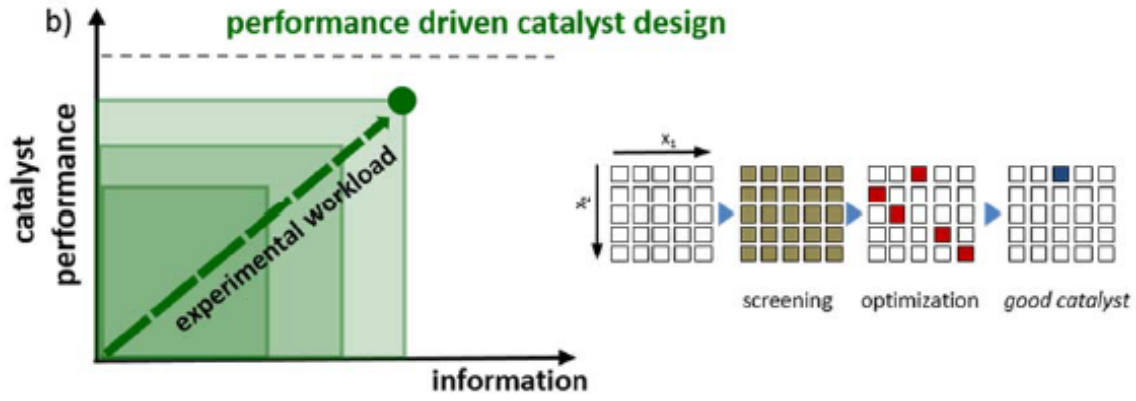

Figure 2.15: Performance-Driven design methodology [4].

Information-Driven Catalyst Design

The Information-Driven technique has the aim to overcome the drawbacks of the previously mentioned methodologies. In this procedure, the first step consists of an initial screening of catalysts to select the catalysts with the properties that better optimize the process and its activity. Still, in this case, the selected ones might not be the most active, but the ones that allow for gathering information on catalyst properties and their performance [4, 47].

The acquisition of this information happens in a second step, where the main objective is to know better the reaction mechanism, especially in terms of intermediates, by-products that can be formed and the effect of operational conditions on the output of the process.

The results of the catalyst screening and testing can be further integrated into a microkinetic model. The needed kinetic and catalytic descriptors for this model are obtained by combining research on a selected catalyst with an exploratory investigation of the catalyst descriptors on a small number of catalysts, accompanied by the initial screening findings [4, 47].

While the kinetic descriptors account for reactive qualities like activity or selectivity in terms of activation energies and pre-exponential factors, the catalytic descriptors account for the impact of catalyst properties on performance. Taking this into account, the catalyst descriptors can be assumed as a fingerprint for the catalyst, that when correlated with the microkinetic model, can translate into different performances [4, 47].

The developed models can then be used to produce reliable simulations by incorporating them into an adequate reactor model to be able to compare simulation with experimental results. This procedure can lead to a very good scale-up of the process while minimizing the number of tests that are done.

Both of the steps in this method require their own high-throughput kinetics set-up, which consists of a set of parallel, usually fixed bed, reactors that are operated at the same temperature and pressure, but with the option of varying space-time and catalysts [4, 47].

The model-driven catalyst design technique or kinetics-driven design is a technique that fits in the information-driven catalyst design method domain [4, 25].

By integrating kinetic modelling with carefully chosen statistical analysis techniques, this method strives to establish the missing descriptor-property connection. It is viewed as a very promising technique that is majorly applied to processes for which finding the optimal catalyst, in terms of activity and stability remains a challenge. Some examples of these successful applications are the OCM and also the production of light olefins via the FTS process [46, 48].

Like any other technique, this approach has a drawback, related to the set of chosen descriptors. If the set of catalyst descriptors is unrealistic, the optimization will not be industrially feasible, thus, the choice of the catalyst descriptors is a very important step of the methodology since it can compromise

all the other stages [46].

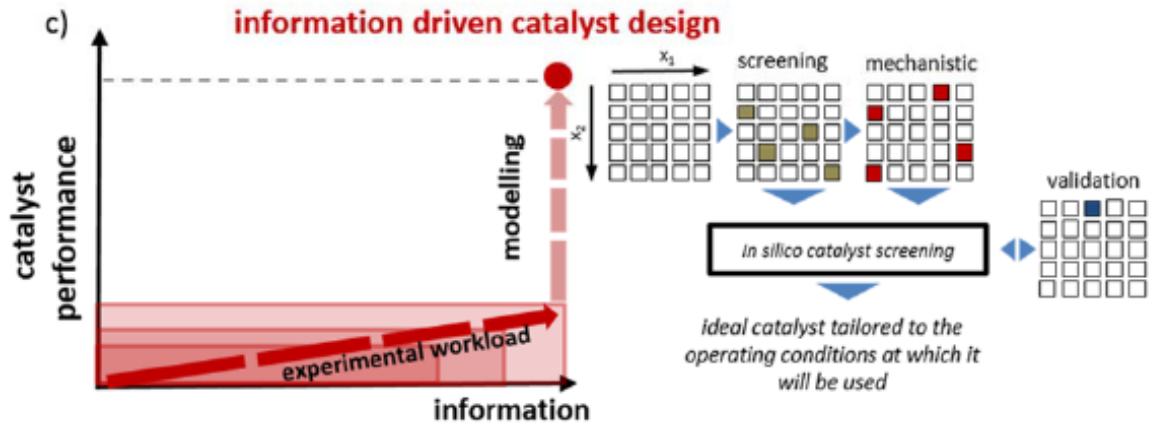

Figure 2.16: Information-Driven design methodology [4].

2.4 Conclusions

Hence, by analysing all the considerations presented in this chapter and reported in the literature, it is possible to conclude that ethylene production is a topic of major importance with several different processes being researched and considered for it in order to help tackle the environmental problems associated to the mainstream production route. As mentioned before, the dehydration of ethanol appears as one of the main ways for this production, especially taking into account the production of ethanol from biomass with similar chemical properties to the one produced from SC, which can address the challenges associated with the process. Nevertheless, the right catalyst for this is still a topic that needs more research, especially concerning problems related to the deactivation of the catalysts, because, in terms of performance, good values for conversion and selectivity have already been obtained.

Following this, the objective of this work is to help this research by applying a MDCD technique to different case studies and consists of an information-driven design technique that allies the kinetics of the process through a microkinetic model where catalyst descriptors will be implemented, together with statistical tests. This aims to establish relationships between the physical properties of the catalyst and the performance so it can be possible to reach an optimal catalyst structure. Considering the reported catalysts, presented previously, zeolites appear as one of the best alternatives since they present very good activity with deactivation being the only downside. So the focus of the work will be on this kind of catalyst, especially, because, on top of what was already mentioned, a larger amount of research on these has already been developed, mainly focusing on the possible modifications to this type of catalyst to improve their stability, so bigger quantities of data on them are reported already making the process of establishing relationships with the physical properties of the materials easier.

3

Methodology

Procedure

Figure 3.1 shows a schematical representation of the methodology proposed in Ref. [46] and followed in this work. Even though the methodology previously presented some issues and some improvements could be made to what was presented in Ref. [46], mainly related to integrating all the methodology in just one software, it was followed equally to how it was stated in the referred work. It is based on three different concepts. The first one is the concept of virtual catalyst which is a computational representation of materials that are defined as a vector of *m* catalyst descriptors ($D_{i,j}$). The number of virtual catalysts to be tested is defined as *n*. The second concept is one of the real catalysts that are materials with known composition and structure and have already been studied, previously, hence their performance is already available and quantified. The third concept on which the methodology relies is the concept of catalyst descriptor. This works as a bridge between virtual and real catalysts being defined as a factor that has an impact on the reaction behaviour and kinetics varying from catalyst to catalyst [46].

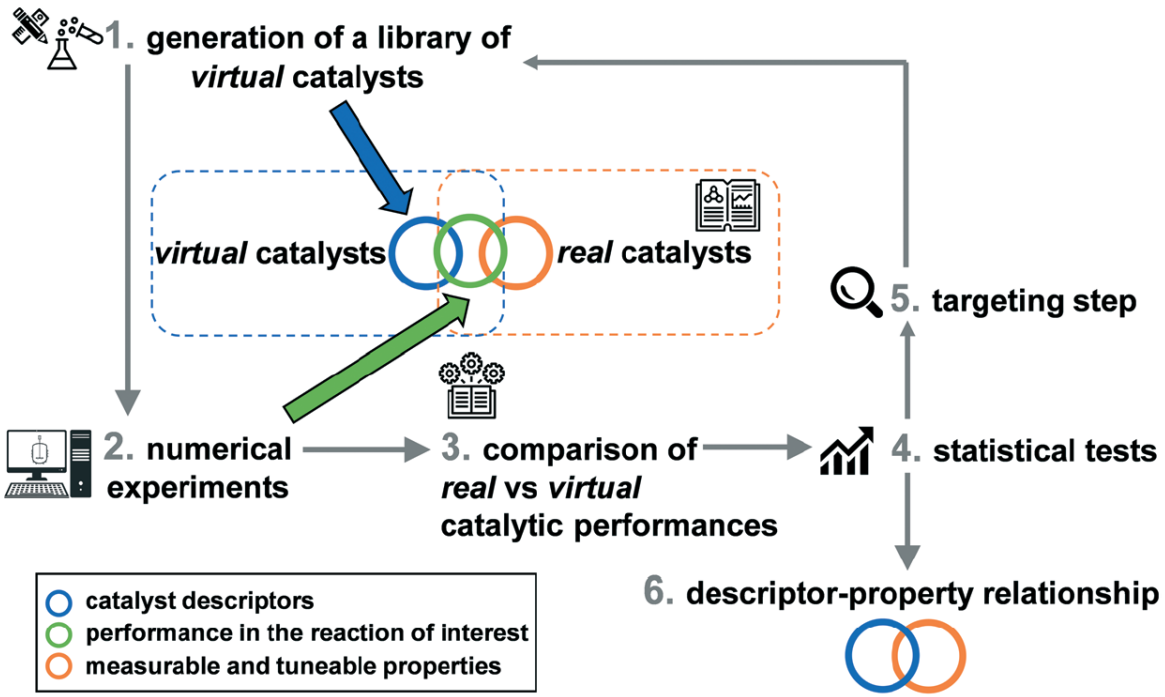

Figure 3.1: Summary of the followed methodology for the model-driven catalyst design technique [46].

The first step in this methodology is the generation of the discovery library of virtual catalysts, in the first iteration, which consists of a set of *n* virtual catalysts. This first library of virtual catalysts is supposed to be very diverse to have a wide range of catalytic performances to be assessed. The first goal of this iterative procedure is to form a targeted library starting from the discovery library, following the steps shown in Figure 3.1. The targeted library consists of the virtual catalysts whose performances are close to the ones of real catalysts, thus it contains only selected catalysts from the discovery library.

If the targeted library can be generated then relationships between the descriptors and the performance itself can be developed [46].

This methodology comprises 6 different steps, which are:

1. Virtual catalysts generation
2. Numerical experiments
3. Comparison between the performances of virtual and real catalysts
4. Analysis of the descriptor distributions
5. Building targeted libraries of catalysts
6. Developing descriptor-property relationships from real catalysts properties

These different steps will now be briefly explained.

Step 1.Virtual catalysts generation

This first step has as its main objective to generate the library of virtual catalysts. As said before, in the first iteration the discovery library is developed, while on further iterations, if that is the case, the targeted library is built.

These virtual catalysts can be generated through several techniques. The preferable ones according to some reports [46] are the DoE, which assures that the sample of virtual catalyst is statistically significant and meaningful, not just a set of randomly generated numbers. Among these statistical techniques, space-filling design is very practical, since it makes good combinations when applied to deterministic systems with a lot of variables as in this case. Space-filling designs are commonly used in computational experiments with the main objective of investigating the link between a set of inputs and a set of outputs generated by a computer simulation [49].

In this methodology, a fast flexible space-filling design was used. This consists of an algorithm that can quickly create space-filling designs both for rectangular and non-rectangular design spaces. When compared to other methods, this Fast Flexible Filling (FFF) designs are able to issue better coverage over the entire design space while being more quick and robust [49]. To apply this method software like JMP 16 can be used [50].

The n virtual catalysts are constituted by a set of m descriptors, leading to a $n \times m$ matrix, as represented by Figure 3.2, where columns represent different descriptors, while rows represent vectors of descriptor combinations that can be called a virtual catalyst.

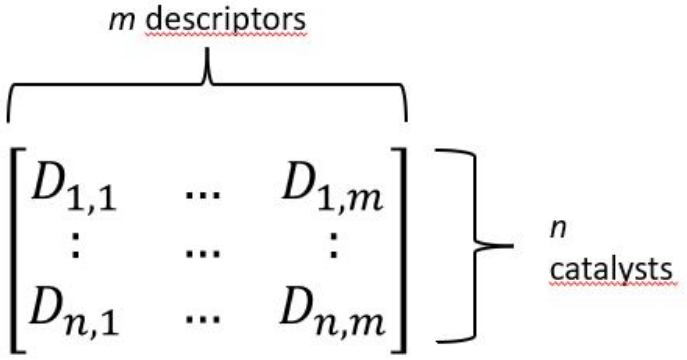

Figure 3.2: General representation of a matrix of catalysts

In terms of values for these descriptors, they should be coherent with the chemistry of the reaction of interest and preferably taken from previous studies that are reported in the literature. More complex reaction systems, involving numerous components usually lead to more catalyst descriptors needed to be taken into account while formulating a virtual catalyst, and *vice versa* [46].

Step 2.Numerical experiments

In this step, the previously generated virtual catalysts, are screened in a numerical set-up. The numerical set-up in this context represents a microkinetic model, where the kinetics is correlated to the selected descriptors, coupled with the adequate reactor model. With this numerical set-up, the behaviour of all virtual catalysts, that compose the discovery library, can be evaluated, and parameters that can characterize catalysts' performance like conversion or selectivity can be calculated [46].

So evaluated performance of virtual catalysts should be further compared to the performance of real catalysts. This, of course, implies that the operating conditions used in the experimental campaign have to be used in the simulation.

Another important factor in this step is to provide enough diversity to the catalyst properties and operating conditions, to be able to identify and quantify their effect on the performance and thus achieve the main goal of the methodology during step 6 [46].

Figure 3.3 displays a graphic representation of this step, where *l*, represents the number of performance parameters taken into account.

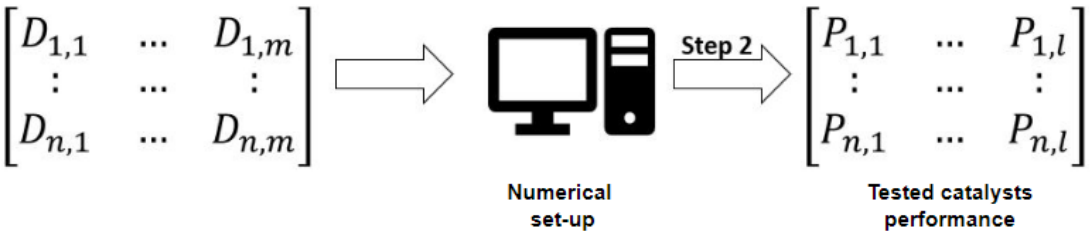

Figure 3.3: Graphic representation of step 2 of the presented methodology.

Step 3.Comparison between the performances of virtual and real catalysts

Once the performance of the virtual catalysts is obtained from the numerical experiments step, it should be compared with the performance obtained with real catalysts. One way of achieving this is by comparing them through clustering algorithms and more precisely the *k-Means* clustering technique [46].

A cluster consists of data points, simulated and/or experimental, that have been grouped due to particular commonalities [51], such as the obtained conversion and selectivities for the studied reaction.

K-means clustering consists of an algorithm based on a centroid where the distance between each point of the studied data set and the centroid is calculated to assign data to a cluster. It can be considered as an iterative process where points will be assigned to a group based on their similarities, in this case, these are the catalyst performances, as represented in Figure 3.4 [52].

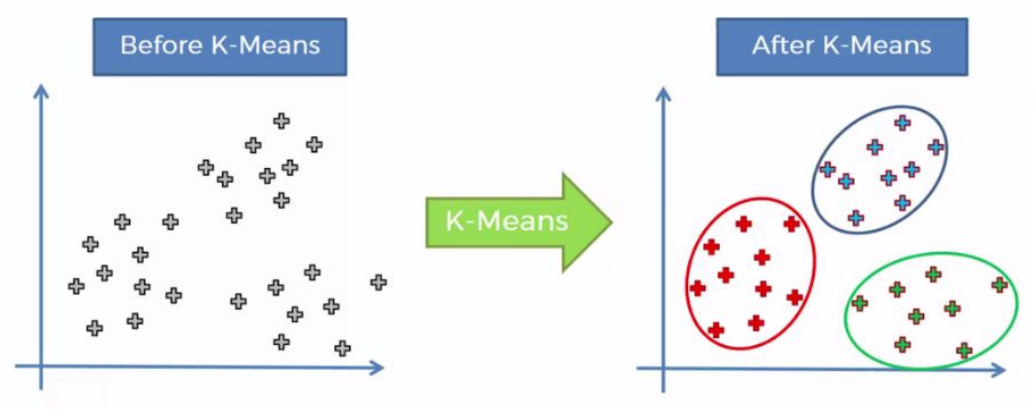

Figure 3.4: Example of the *k-means* clustering technique [53].

In the end, the main objective is to minimize the sum of the distances between the centroid and the studied data points [52].

For this purpose, the software *Orange3* [54] was utilized. This consists of a very intuitive tool that can assess some problems related to *k-Means* clustering, namely the choice of a correct number of clusters for a specific dataset and the high influence on the obtained results of the initialization step of

the method [55, 56].

Concerning the first problem, the software overcomes it by using the Silhouette evaluation to assess the ideal number of clusters (k). Silhouette can be considered as a measure of similarity and works by analysing the distance of each data point to the cluster where it belongs and its closest cluster, which can be defined as the average distance of a point to all the remaining ones within the cluster and that to all the points in the closest cluster. Then the silhouette value for a clustering technique can be considered the average of the silhouette values for all the points involved [57]. The number of clusters that present higher silhouette values represents the ideal cluster subdivision for a dataset.

Regarding the second issue with this technique, the initialization method utilized by this *software* is the *K-means ++*. This starts by spreading out the first centroid randomly and then selecting the other ones relying on the maximum square distance concept, as can be seen in eq. (3.1), where x_i is a data point and C_j a centroid [52]. Basically, after randomly picking the first centroid, it calculates the distances between all the data points and the centroid. The datapoint that verifies eq. (3.1) will be considered as a new centroid and the process is repeated until all the clusters are defined [52].

$$D_i = max_{(j:1-k)} \| X_i - C_j \|^2 \tag{3.1}$$

Step 4.Statistical analysis of the descriptor distributions

This fourth step is one of the most relevant ones since it is the one that will allow us to understand the real influence of some descriptors on the observed performances.

The descriptors present different probability distributions in each one of the clusters obtained before. By taking this concept into account, through comparing these distributions within all the clusters, we can get to the more relevant descriptors, which allows us to differentiate from one to the other and start to relate these with some real properties already [46].

To test the descriptor distributions some specific statistical tests need to be applied. In this case, tests like the ANOVA or the t-student test, which are the most commonly used ones, should not be applied, as these are indicated for data that follows a normal distribution type and catalyst descriptors are likely to be non-normally distributed within the different clusters. Thus the non-parametric alternatives of the mentioned tests, like the Kruskal-Wallis and the Mann-Whitney test, should be used [46].

The Kruskal-Wallis test by definition is used to determine if there is a difference that can be statistically significant between the medians of three or more groups, in this case, clusters [58].

In the case of the Mann-Whitney test, it is an equivalent of the two-sample t-student test, with the difference that while the t-student test makes assumptions about the population's distribution, the Mann-Whitney test makes no assumptions [59]. This test is applied in the case where the number of clusters to be studied is equal to 2.

The assessment parameter that will be used in the application of this statistical test to evaluate if a descriptor is a discriminating one or not will be the p-value. This value allows us to reject or evince the null and the alternative hypothesis. The alternative hypothesis defends that the observed results have an influence that is not a random cause while the null hypothesis defends that it occurs randomly. Hence, if the p-value is under a certain threshold one can reject the null hypothesis and consider the alternative hypothesis as the correct one. If the value is higher, one cannot reject the null hypothesis and cannot conclude anything about the correctness of the alternative one [60]. For the studied methodology, the p-value considered as the threshold for the identification of a descriptor as relevant or not was 0.05 as it was already proven to be a good limit [61]. This means that if the distribution of a determinate descriptor within the clusters presented a p-value lower than 0.05 it is considered relevant.

As in step 1, this test can also be applied by using the JMP 16 software [50].

Step 5.Building targeted libraries of catalysts

To accomplish the methodology's objective, and to be able to establish relationships between catalyst descriptors and physical properties, the number of virtual catalysts close to real catalysts should be high enough. For this, the number of virtual catalysts in the surrounding of real catalysts should be increased across iterations, which is done by generating targeted libraries from the discovered library used in the first iteration.

Consequently, targeting means reducing the design space iteratively through the diminishing of discriminating descriptor ranges with the main objective of getting virtual catalysts closer to the performance of real catalysts [46].

There are no specific criteria defining when to stop performing this step. A good indication that there is a representative sample of virtual catalysts is when the number of these virtual catalysts does not increase in a cluster on consecutive iterations [46].

Concerning this narrowing down of the value ranges, standard deviations of around $\pm\sqrt{2}$ times the standard deviations of the discriminating descriptor on the studied cluster can be applied to the mean of the cluster being studied by using eq. (3.2). It is reported, according to Chebyshev inequality that by applying this formula, at least 50% of the virtual catalysts are retained on the new cluster that is being generated [62, 63], as can be proven by eq. (3.3) that represents the Chebyshev theorem where k is the value taken into account as $\sqrt{2}$ for this case.

$$Di_{targeted} = \overline{Di_{discovery}} \pm \sqrt{2} \times \sigma_{discovery} \tag{3.2}$$

$$Chebyshev\,Theorem/inequality = 1 - \frac{1}{k^2} \tag{3.3}$$

Step 6.Developing descriptor-property relationships from real catalysts properties

This step aims at establishing a relationship between a qualitative property, which is measurable and tuneable property of the studied catalyst and the descriptor that reflects this property in the kinetic model(i.e. reflects on the kinetics).

A graphic representation of steps 4 and 6, taken from the paper that served as the basis for the applied methodology [46], is shown in Figure 3.5. It demonstrates how a comparison of descriptors distributions and the identification of the most relevant descriptor is performed, as well as the establishment of a relationship between these and the real properties of catalysts. Firstly, step 4 represents the comparison of the descriptors distributions within two different clusters allowing the differentiation between a cluster with low D_i and high D_i. Considering this, from each one of the two clusters, that present different properties between them, it is possible to take out conclusions by establishing a relation between the values of D_i and the property that characterized the real catalysts present in the cluster, constituting this step 6. From the moment these assumptions are made, a qualitative relationship between a measurable property of a catalyst and the descriptor that represents the role of that catalyst on the observed kinetics is done, which is the final goal of the methodology [46].

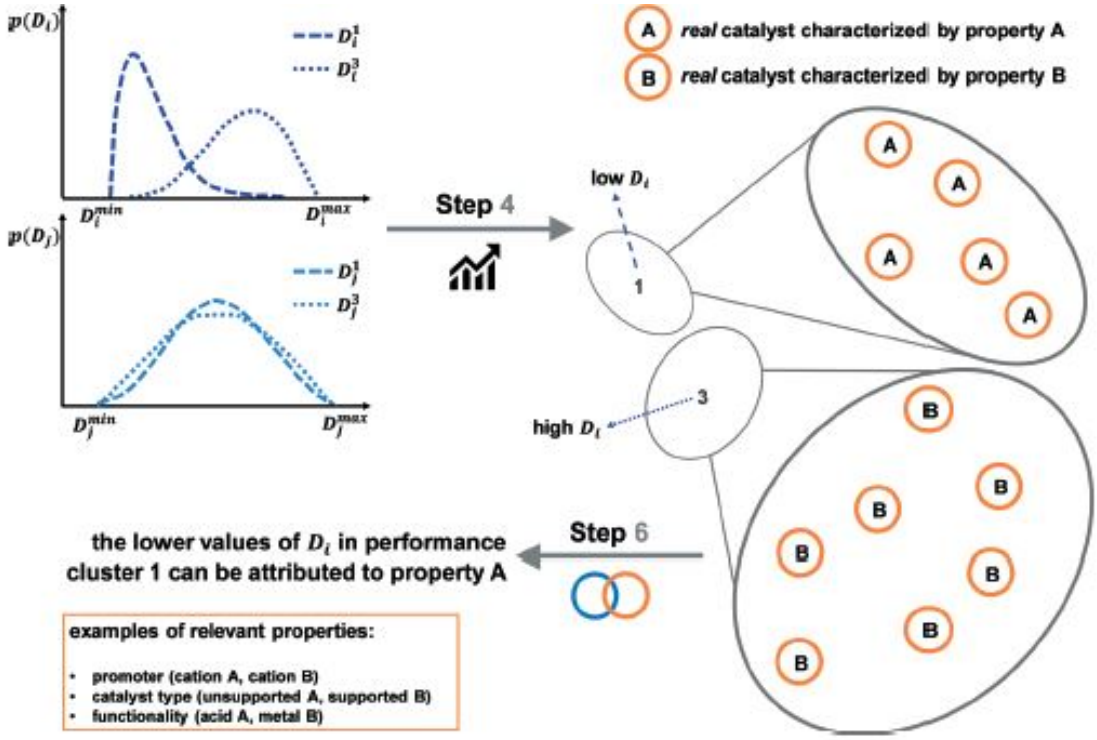

Figure 3.5: Graphic representation of steps 4 and 6 of the presented methodology [46].

4

Catalyst design

Contents

The experimental results of two individual studies from the literature [3,24], reporting the performance of various zeolite-based catalysts in the process of ethanol dehydration to ethylene, have been used in this work. These studies had the main objective of studying the impact of some modifications, mainly metal doping and dealumination processes, on the performance and stability of zeolites and they were the chosen ones because, within their sets of experimental data, zeolites have suffered, exactly, some of these modifications that are considered as some of the most relevant due to their influence on catalysts activity and stability, as presented in chapter 2. On top of that, it was possible to extract the presented data, easily, from the tables reported in the studies, so these were more accurate than if they needed to be extracted by visual interpretation from figures.

The methodology presented in Chapter 3 was then applied to obtain a relationship between the physical properties of the used catalysts and here identified descriptors that bridge these physical properties and their effect on the kinetics of the given reaction. Real catalysts, used in the two selected studies possess different physical properties that were previously well-characterized and studied. The first two steps of the methodology, including the used kinetic model, are common for all the studied experimental datasets. The third step of the methodology is also very similar to all the studied data since the performance assessment parameters and the clustering technique were the same for all of them. Steps 4,5 and 6 are very case study dependant since the statistical tests to be applied and consequent conclusions will depend on the number of clusters obtained and on the real catalysts performance of each study.

4.1 Generation of the virtual catalyst library

As mentioned earlier, a virtual catalyst is a combination of identified descriptors. Accordingly to the relevant reports [46, 48, 64], usually employed catalytic descriptors include: 1) chemisorption enthalpies of components, 2) sticking coefficients or initial probabilities that can be defined as the probability of a molecule to be adsorbed on the catalyst surface after getting trapped [65], and, lastly, 3) the density of active sites of the studied catalysts.

A virtual catalyst is defined by selecting a value for each descriptor from a priory-defined descriptor range based on DoE and FFF methods. The initial set of these virtual catalysts represents the discovery library. The number of virtual catalysts in the discovery library needs to be large enough to have a representative set of descriptors combinations which will allow for establishing a relationship between physical property and performance. With the descriptor number increase, the number of virtual catalysts should increase as well.

As stated earlier the reaction network of ethanol dehydration to ethylene considered in this work is presented in Figure 2.11. Accordingly, as mentioned above, the descriptors chosen in this work were

based on works that were previously developed on this kind of methodology so it is already known that they can influence the kinetics of the process and the way how to implement them on the kinetic model was already reported as well. Considering this, the used ones were the following: 1) the sticking coefficients of ethanol, 2) the sticking coefficient of ethylene, 3) the chemisorption enthalpies of ethanol, 4) the chemisorption enthalpy of ethylene, 5) the chemisorption enthalpy of DEE, and 6) the density of active sites of the used catalyst. The used ranges for these parameters were estimated based on a literature survey and their values are presented in Table 4.1. In the case of sticking coefficients, due to a lack of data in the literature, their initial range was considered to be between 0 and 1 since they represent probabilities.

The density of active sites was initially calculated by making use of the Horvath-Kawazoe method [24], shown by eq. (4.1). The density of active sites is given in mol/m^2, while the acid amount is mol/g and the BET surface area is in m^2/g. Applying the FFF design method, a discovery library was generated in this work containing 120 virtual catalysts represented by a combination of those 6 descriptors. This discovery library is presented in Table A.1 in appendix A. Figure 4.1 represents a 2D visualization of the resulting discovery library, where each point represents a virtual catalyst.

$$\rho_{acidactivesites} = \frac{Total\,acid\,ammount}{BET_{SurfaceArea}} \tag{4.1}$$

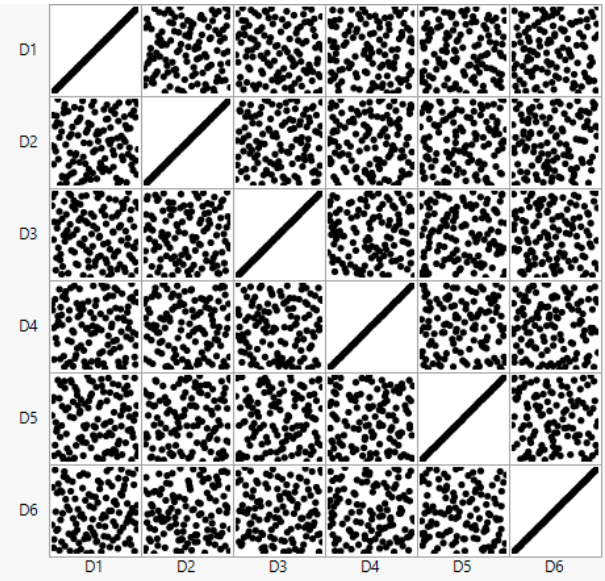

Figure 4.1: Scatterplot matrix representation for the obtained discovery library by application of the FFF design. Where D1,D2 and D3 represent the chemisorption enthalpies of ethanol,ethylene and DEE, respectively. D4 and D5 represent the sticking coefficients for ethanol and ethylene and, lastly, D6 is the density of active sites.

Table 4.1: Value ranges used for the catalyst descriptors in the discovery library

Descriptor	Value
$\Delta H_{chemisorption,Ethanol}$ (kJ/mol)	35-135 [66–68]
$\Delta H_{chemisorption,Ethylene}$ (kJ/mol)	35-165 [69]
$\Delta H_{chemisorption,DEE}$ (kJ/mol)	50-90 [70]
$S_{0,Ethanol}$	0-1
$S_{0,Ethylene}$	0-1
$\rho_{active\ sites}$(mol/m^2)	2×10^{-7} - 2×10^{-6} [24, 71]

4.2 Kinetic Model

4.2.1 Model formulation

To develop a microkinetic model, the reaction mechanism is the first thing that needs to be specified. A microkinetic model is always coupled to a reactor model to be able to compare the simulation and experimentally obtained results. Therefore, a kinetic model is usually defined by a group of mass balance equations that take into account the thermodynamic and kinetic properties of the system.

In this study, a microkinetic model was developed by using the reaction mechanism shown in Figure 2.11 with the elementary steps presented in Table 2.2.

Based on this, a joint Langmuir-Hinshelwood-Hougen-Watson (LHHW) and Eley-Rideal (ER) mechanism was employed.

The LHHW approach defends that the adsorption of both reactants happens before the surface reaction. It relies on some assumptions [72]:

- Entire surface presents the same activity for chemical adsorption
- Coverage does not influence the adsorption rate
- One species can only adsorb on one active site
- The adsorption species are all identical
- Molecules only adsorb on free sites

ER mechanism, on the other side considers that at least one of the reaction species participating in one reaction reacts from the gas phase, while others react as adsorbed species [73].

Adsorption and desorption rates of a species *i* that undergo adsorption/desorption, apart from steps 1,5 and the forward step of reaction 9, where descriptors were implemented, were calculated according to eq. (4.2) and eq. (4.3), respectively regardless of the model assumed for a specific reaction (LHHW or ER). $k_{i,ads}$, θ^*,$p_{i,g}$, θ_i stand for the adsorption rate coefficient, partial pressure of component *i* in the

gas phase, the fraction of free active sites, desorption rate coefficient and the coverage of active sites by component *i* in the same order.

$$r_{i,ads} = k_{i,ads} \times p_{i,g} \times \theta^* \tag{4.2}$$

$$r_{i,des} = k_{i,des} \times \theta_i \tag{4.3}$$

The rates of reactions that follow ER mechanism were described by eq. (4.4) where $k_{r,ER}$ represents the reaction rate coefficient of the surface reaction *r* (index ER indicates that reaction is taking place according to ER mechanism), while p_i indicates the partial pressure of the component *i* that reacts from the gas phase. On the other side, if the reaction follows the LHHW mechanism the rate of surface reaction *r* was calculated according to eq. (4.5), where $k_{r,LHHW}$ stands for the reaction rate coefficient (index LHHW indicates that reaction is taking place according to LHHW mechanism), and θ_j denotes surface coverage by component *j* (another reactant apart from the reactant *i*).

$$r_{r,ER} = k_{r,ER} \times \theta_i \times p_{i,g} \tag{4.4}$$

$$r_{r,LHHW} = k_{r,LHHW} \times \theta_i \times \theta_j \tag{4.5}$$

Finally, the balance of active sites is needed to simply account for the amount of vacant active sites available for adsorption at any given moment. θ^* has been calculated by eq. (4.6), where $\theta^*{}_0$ denotes the initial amount of active sites which is equal to 1 as being related to the fraction. Accordingly, the surface coverage available in a given time is a difference between the total (initial) amount of active sites and all occupied active sites (occupied active sites correspond to the sum of surface coverages by all adsorbed species).

$$\theta^* = \theta_0^* - \sum_{i=1}^{N} \theta_i \tag{4.6}$$

The kinetic model was built around two assumptions:

- No rate determining step (RDS) consideration;
- Pseudo steady-state was considered for the surface species.

This further means that the rate of all reactions is calculated and that the concentration of surface species does not change in time [74].

A plug-flow fixed bed reactor was used to collect experimental data in both case studies. Therefore the mass balance of the components in the gas phase was calculated according to eq. (4.7), which is

an ordinary differential equation. As such it needs one initial condition to be numerically solved, which in this case was that $F_i = F_{i,0}$ at $W = 0$ (F_i and $F_{i,0}$ stands for the flowrate of component *i* along the catalyst bed and the flowrate of component *i* at the reactor inlet in mol/s, respectively, while *W* stands for the catalysts mass in kg). Following the assumption of steady-state for the surface species, the mass balance on the catalyst's surface was calculated, therefore, according to eq. (4.8), which is an algebraic equation. Table 4.2 summarizes all the steps and respective thermodynamic parameters which were used for the calculation of the kinetic constants, namely the ones for activated steps, following van't Hoff and Arrhenius equations, to be further used on the kinetic model.

$$\frac{dF_i}{dW_{cat}} = R_i = C_t \times (\sum_{1}^{N} r_{i,ads} - \sum_{1}^{N} r_{i,des} \pm \sum_{1}^{N} r_{i,reaction}) \tag{4.7}$$

$$\frac{d\theta_k}{dt} = 0 = \sum_{1}^{N} r_{k,ads} - \sum_{1}^{N} r_{k,des} \pm \sum_{1}^{N} r_{k,reaction} \tag{4.8}$$

Table 4.2: Standard reaction enthalpy (kJ/mol), standard reaction entropy (J/mol/K), activation energy (kJ/mol) and pre-exponential factor (s^{-1} or 10^{-2} kPa^{-1} s^{-1}) of forward reaction, forward reaction rate coefficient kf (s^{-1} or 10^{-2} kPa^{-1} s^{-1}) at 500 K and equilibrium coefficient at 500 K (10^{-2} kPa^{-1}, 10^{-2} kPa or dimensionless for adsorption, desorption and surface transformation, respectively) for the elementary steps [39].

	Elementary Steps	ΔH_r^0	ΔS_r^0	E_a(f)	A_f	k_f (500K)	K_{eq} (500K)
(0)	$W \leftrightarrow H_2O(g) + *$	83	151	-	-	-	$1.7 \cdot 10^{-1}$
(1)	$EtOH(g) + * \leftrightarrow M1$	-122	-167	-	-	-	$1.1 \cdot 10^{4}$
(2)	$M1 \leftrightarrow M2$	14	7	-	-	-	$8.0 \cdot 10^{-2}$
(3)	$M2 \leftrightarrow ethoxy + H_2O(g)$	77	146	118	$4.0 \cdot 10^{13}$	$1.9 \cdot 10^{1}$	$3.8 \cdot 10^{-1}$
(4)	$Ethoxy \leftrightarrow Ethene*$	44	60	106	$9.4 \cdot 10^{12}$	$7.9 \cdot 10^{1}$	$3.5 \cdot 10^{-2}$
(5)	$Ethene* \leftrightarrow C_2H_4(g) + *$	48	99	-	-	-	$1.4 \cdot 10^{0}$
(6)	$M1 + EtOH(g) \leftrightarrow D1$	-99	-162	-	-	-	$7.6 \cdot 10^{1}$
(7)	$D1 \leftrightarrow D2$	44	24	-	-	-	$4.5 \cdot 10^{-4}$
(8)	$D2 \leftrightarrow DEE* + H_2O(g)$	16	125	92	$3.5 \cdot 10^{12}$	$8.6 \cdot 10^{2}$	$7.2 \cdot 10^{4}$
(9)	$DEE* \leftrightarrow DEE(g) + *$	139	165	-	-	-	$1.3 \cdot 10^{-6}$
(10)	$DEE* \leftrightarrow C1$	114	51	145	$4.6 \cdot 10^{13}$	$3.3 \cdot 10^{-2}$	$5.7 \cdot 10^{-10}$
(11)	$C1 \leftrightarrow Ethene* + EtOH(g)$	59	175	-	-	-	$9.5 \cdot 10^{2}$
(12)	$Ethoxy + EtOH(g) \leftrightarrow DEE*$	-129	-166	18	$4.3 \cdot 10^{4}$	$5.7 \cdot 10^{2}$	$6.4 \cdot 10^{4}$
(13)	$D2 \leftrightarrow C2 + C_2H_4(g)$	57	131	110	$3.8 \cdot 10^{12}$	$1.2 \cdot 10^{1}$	$7.7 \cdot 10^{0}$
(14)	$C2 \leftrightarrow M1 + H_2O(g)$	59	152	-	-	-	$6.0 \cdot 10^{1}$
(15)	$M1 \leftrightarrow W + C_2H_4(g)$	99	161	180	$5.1 \cdot 10^{14}$	$8.0 \cdot 10^{-5}$	$1.2 \cdot 10^{-2}$
(16)	$M2 \leftrightarrow C3$	83	63	129	$1.9 \cdot 10^{13}$	$6.4 \cdot 10^{-1}$	$4.2 \cdot 10^{-6}$
(17)	$C3 \leftrightarrow W + C_2H_4(g)$	2	92	-	-	-	$4.0 \cdot 10^{4}$
(18)	$W + EtOH(g) \leftrightarrow C2$	-98	-169	-	-	-	$2.6 \cdot 10^{1}$
(19)	$C2 \leftrightarrow 2W + C_2H_4(g)$	77	151	175	$1.2 \cdot 10^{15}$	$6.3 \cdot 10^{-4}$	$7.0 \cdot 10^{-1}$
(20)	$2W \leftrightarrow W + H_2O(g)$	81	162	-	-	-	$1.0 \cdot 10^{0}$

The pseudo-steady state approximation resulted in a system of Differential Algebraic Equation (DAE). To solve this kind of equations Python was used by making use of the *numpy* and *scipy* packages [75].

Adsorption rate coefficients for the non-activated adsorption steps, namely steps 0,6,11,14,17,18 and 20 were calculated based on the collision theory as eq. (4.10) indicates [76]. Reaction rates for the remainder of the non-activated steps were calculated based on transition-state theory as eq. (4.9) indicates [39, 77]. The desorption rate coefficient was calculated by applying thermodynamic consistency [39, 77]. Finally, the rate coefficients of steps 1, 5 and 9 were calculated taking into account previously defined descriptors as it will be explained in section 4.2.2. In the respective equations (eq. (4.9)-eq. (4.10)), k_B stands for Boltzmann constant, *m* the mass of a molecule, *h* represents the Planck's constant, N_0 the number of reaction sites per catalyst and *T* the temperature in Kelvin.

$$k_{ads} = \frac{k_B T}{h} \tag{4.9}$$

$$k_{ads} = \frac{1}{N_0 \sqrt{2\pi m k_B T}} \tag{4.10}$$

$$k_{des} = \frac{k_{ads}}{K_{eq}} \tag{4.11}$$

The resulting model appeared to be very stiff as the kinetic parameters varied several order of magnitude among each other. This created numerical instability which needed to be neutralized to be able to obtain any meaningful solution. This is a rather common situation when considering LHHW and/or ER mechanism and microkinetics, nonetheless possibilities to address this issue should be evaluated for each given system. In this work, several options have been considered such as using different DAE solving algorithms and adjusting the step size. Additionally, a scaling factor of 10^3 for the non-activated step rates was used to cope with this issue, which also proved to be the most effective. The reasons for introducing this scaling factor were two-fold. First, the same scaling factor was also applied in the previous study on the system [78]. Second, it was assumed that the reduction of the rate coefficients for three orders of magnitude would not compromise the balance between adsorption/desorption and reaction rate, i.e. that the reaction will still be a sufficiently slower process. Apart from the scaling factor, it might be worth noting that the model was initially based on the component concentrations, however, it was observed that working with the coverages provided better numerical stability, thus the rates formulated in terms of coverages were used as the final model version.

The used parameters to assess the catalyst's performance were the conversion of ethanol and the selectivity to ethylene and diethyl ether. These were calculated by making use of eq. (4.12), eq. (4.13) and eq. (4.14), respectively, with the flows in mol/s.

$$X = \frac{F_{Ethanol,0}}{F_{Ethanol,0} - F_{Ethanol,final}} \tag{4.12}$$

$$S_{Ethylene} = \frac{F_{Ethylene,final}}{F_{Ethanol,0} - F_{Ethanol,final}} \tag{4.13}$$

$$S_{DEE} = \frac{2 \times F_{DEE,final}}{F_{Ethanol,0} - F_{Ethanol,final}} \tag{4.14}$$

4.2.2 Descriptor implementation

The above-mentioned 6 descriptors were implemented in the model via rate coefficients. The adsorption and desorption steps of the gaseous species C_2H_4, DEE, and C_2H_5OH were the chosen ones for descriptor implementation, namely steps 1,5 and the desorption step in 9 as shown in Figure 2.11. These descriptors were used in this work due to: i) these were typical descriptors considered in other works [46, 64] and ii) because these were the ones for which finding data on their value ranges was easier. Adsorption steps were assumed to be non-activated ones, thus the rate coefficient was calculated via eq. (4.15) [64], where k represents the rate constant of the reaction, $S_{0,i}$ is the initial sticking probability, n is the order of the reaction, R is the universal gas constant and, lastly, M is the molar mass of the adsorbed component in kg/mol. This equation was then converted to pressure units so it could be used in the model by making use of the ideal gas law [79].

$$k = \frac{S_{0,i}}{\sigma^n} \sqrt{\frac{RT}{2\pi M}} \tag{4.15}$$

The rate coefficients of desorption steps were calculated by making use of the Arrhenius equation, presented as eq. (4.16) [64], where, A is the pre-exponential factor, that was assumed to be placed in the interval from 10^{13} s^{-1} to 10^{16} s^{-1} as proposed by James A. Dumesic *et al.* [80]. Lastly, E_a represents the activation energy of the reaction step in J/mol.

The activation energies of these desorption steps were considered equal to the respective chemisorption enthalpies of the different species. This is based on the assumption that these steps are non-activated, as mentioned before, so the activation energies can be considered zero.

$$k = A \times \exp\left(\frac{-Ea}{RT}\right) \tag{4.16}$$

4.3 Results and discussion

4.3.1 Case Study 1

The experimental dataset studied by N.Zhan *et al.* [24] was selected in this work to perform MDCD. In their work, a set of 6 different HZSM-5 zeolites, pure and doped with lanthanum and phosphorous, were

tested under different operational conditions. The used percentages of each element were 0.25%,0.5% and 1% for lanthanum and 2% for phosphorous.

Table 4.3 shows the list of used catalysts with the indicated percentage of lanthanum and phosphorous in the doped ones as well as the respective conversions of ethanol and ethylene selectivities achieved. Table 4.4 provides information about obtained catalyst characterization results.

Table 4.3: Real catalysts and respective performances for dataset 1 [24].

Catalyst	$X_{Ethanol(\%)}$	$S_{Ethylene}$ (%)
HZSM-5	87.3	83.9
2%PHZSM-5	73.5	15.8
0.25%La-2%PHZSM-5	78.5	22.8
0.5%La-2&PHZSM-5	88.2	30.6
1%La-2%PHZSM-5	76.9	32.1
0.5%LaHZSM-5	89.7	85.0

Reaction condition:0.5g of catalyst, atmospheric pressure, WHSV = 2.0h^{-1}.

Table 4.4: Characteristics of the HZSM-5 zeolite and its modified versions on dataset 1 [24].

Catalyst	S_{BET} (m^2 g^{-1})	V_{micro} (cm^3 g^{-1})	Pore width (nm)
HZSM-5	253	0.14	0.5615
2%PHZSM-5	187	0.13	0.5476
0.25%La-2%PHZSM-5	192	0.14	0.5489
0.5%La-2&PHZSM-5	194	0.14	0.5496
1%La-2%PHZSM-5	211	0.15	0.5665
0.5%LaHZSM-5	297	0.17	0.5623

Step 2-Numerical experiments

Upon the generation of the discovery library in section 4.1, all the virtual catalysts were tested *in silico*(by the mean of a microkinetic model) and the obtained performances have been displayed in Figure 4.2, which shows ethylene selectivity as a function of ethanol conversion.

The real catalysts performance is also presented in Figure 4.2 for an easier evaluation of virtual ones in terms of matching the real catalyst behaviour.

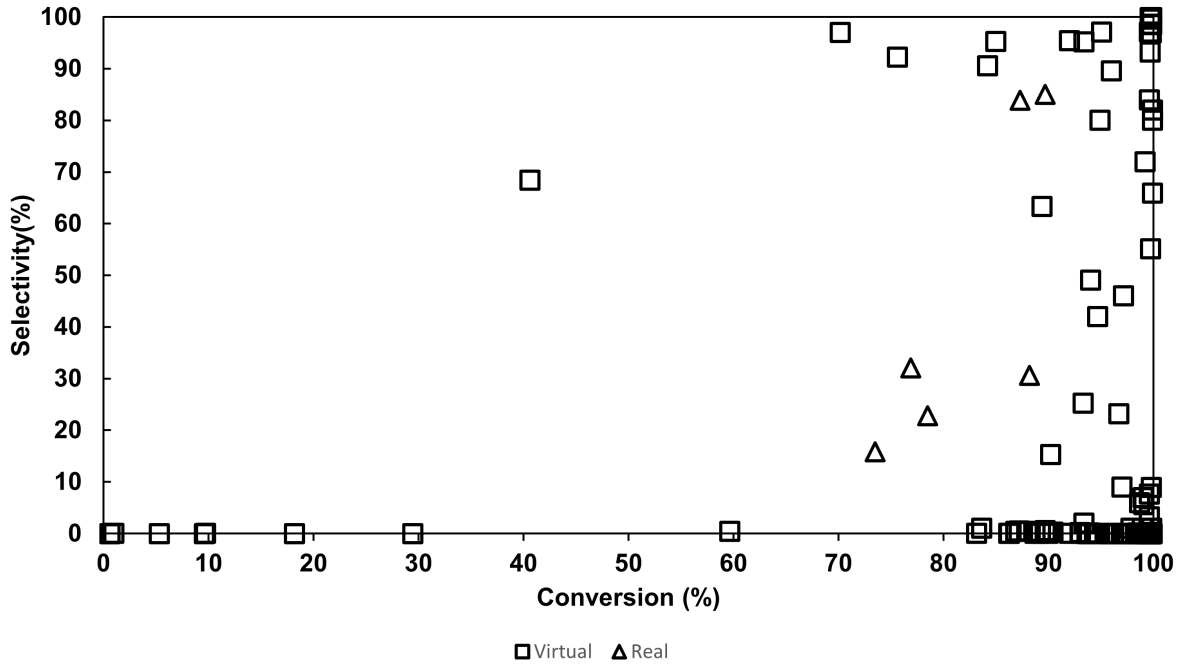

Figure 4.2: Obtained performances for the simulated virtual catalysts and the respective real catalysts from dataset 1.Reaction conditions:T=493K, W=0.5g of catalyst, atmospheric pressure, WHSV = 2.0h^{-1}.

Step 3- Comparison between the performances of virtual and real catalysts

By making use of the *Orange3* software to statistically evaluate the match between virtual and real catalysts, three different clusters were identified for all the performances obtained with virtual and real catalysts as the ideal number of division groups, as shown in Figure 4.3. The first cluster, coloured in blue, corresponds to very low conversion and selectivity. The second one, coloured in orange, corresponds to high conversions associated but lower selectivities. Lastly, the third cluster in yellow presents high selectivities and conversions. Figure 4.3 is accompanied by Table 4.5, which shows details about each cluster. Given that only clusters, number two and three have both virtual and real catalysts these two are the only relevant clusters that will be statistically studied in further steps.

Table 4.5: Description of the three obtained clusters by application of k-means clustering technique to the discovery library of case study 1.

Cluster	Colour	Number of real catalysts	Number of virtual catalysts	$X_{Ethanol}$(%) (mean and standard deviation)	$S_{Ethylene}$(%) (mean and standard deviation)
C1	Blue	0	9	12.79±14	7.61±23
C2	Orange	4	83	95.00±7	3.04±8
C3	Yellow	2	28	94.66±8	86.07±16

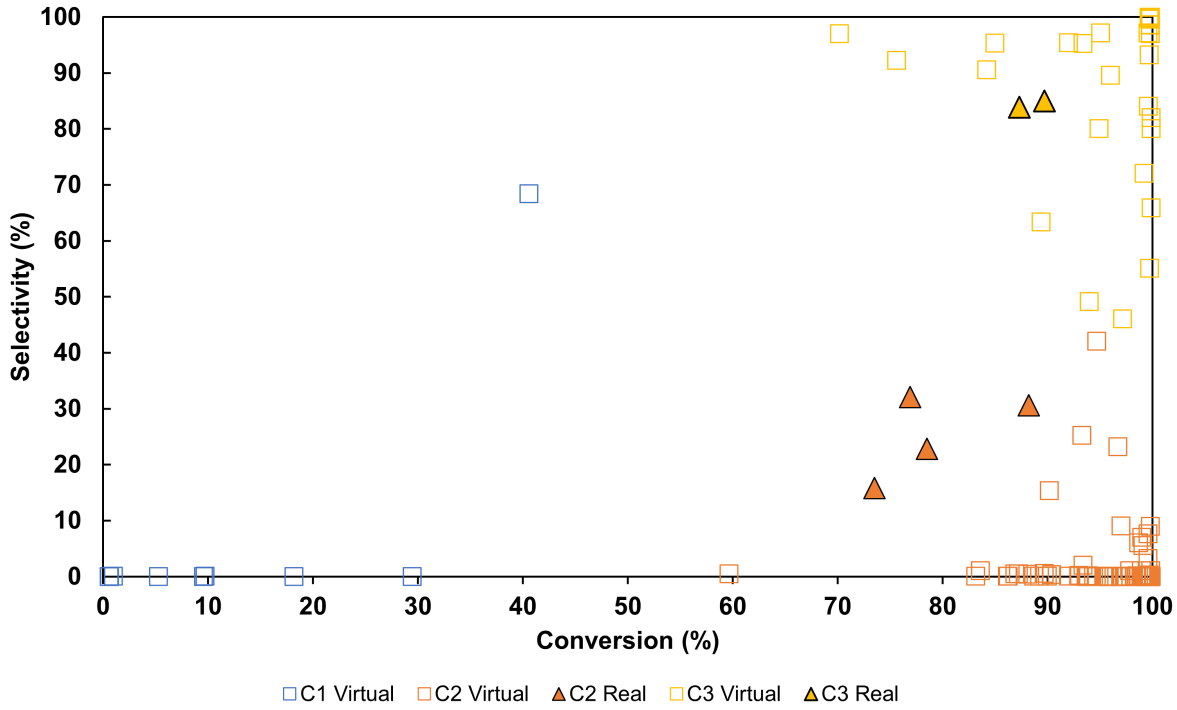

Figure 4.3: Output of the clustering step performed in *Orange3* for case study 1.

Step 4- Statistical analysis of the descriptor distributions

After applying the statistical tests described in chapter 3, the relevance of used descriptors for observed catalyst behaviour has been assessed by using the p-value of the statistical tests as a quantitative criterion. Table 4.6 summarizes the p-values obtained for all descriptors used in this step. Descriptors with p-value lower than 0.05 were considered relevant.

Accordingly, only the chemisorption enthalpy of ethylene satisfied this criterion and was thus identified as the most influential descriptor for the obtained results. Figure 4.4 displays a comparison between the distributions of this descriptor in boxplots, where the central line of the box represents the median of the descriptor distribution within the cluster, the cross represents the mean for the descriptor values in each cluster, and the edges of the box represent the 25th percentile when at the bottom and 75th percentile at the top. The lines that stand outside the box are the respective standard deviations of each one of the clusters. These box plots work as a very good tool when several groups of data are being studied simultaneously [81]. Because, not only this representation can already help establish relationships since it is already possible to see a trend in terms of cluster 2 presenting higher values of chemisorption enthalpy, while cluster 3 presents very lower chemisorption enthalpy values, but also it proves that the descriptors are not normally distributed, otherwise the median would be centred inside the box and the rest of the diagram would be symmetric, proving what was said in chapter 3, regarding

the application of non-parametric statistical tests.

Table 4.6: Results of the statistical tests applied to each descriptor

Descriptor	p-value
$\Delta H_{chemisorption,Ethanol}$	0.85
$\Delta\ H_{chemisorption,Ethylene}$	$<$0.001
$\Delta H_{chemisorption,DEE}$	0.3
$S_{0,Ethanol}$	0.78
$S_{0,Ethylene}$	0.35
$\rho_{active\ sites}$	0.08

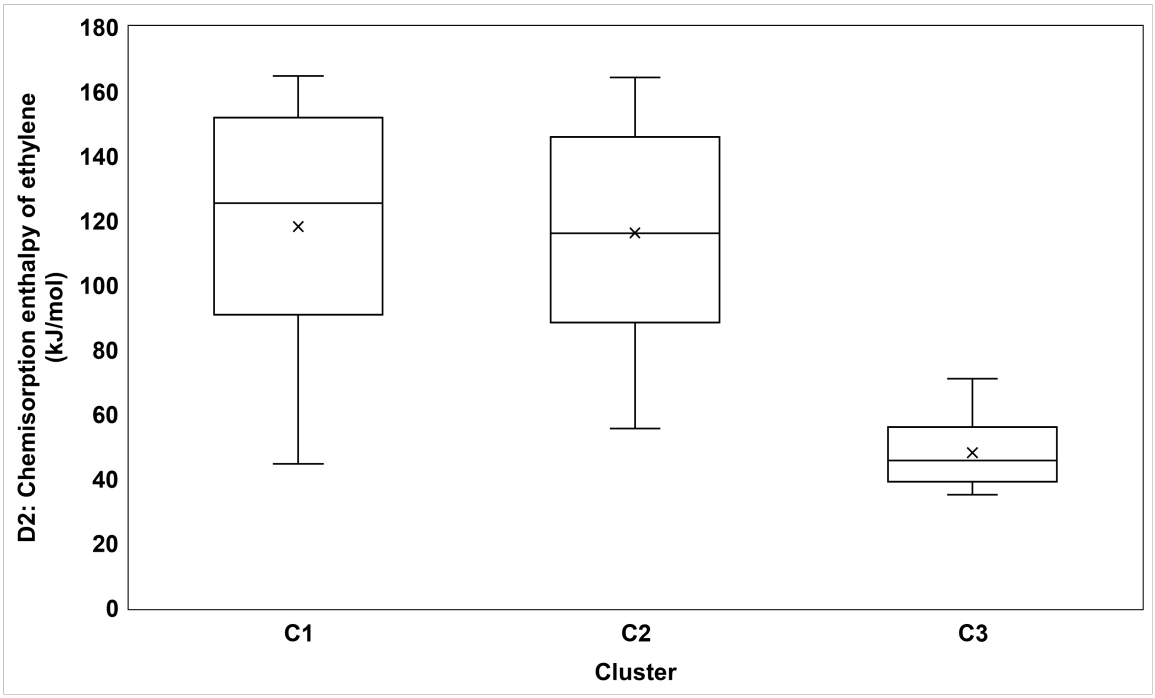

Figure 4.4: Comparison of the distributions of the relevant descriptor between clusters for the discovery library of case study 1.

Figure 4.5 proves what was just mentioned as it shows a representation of the probability density function for the chemisorption enthalpy of ethylene and it is very non-identical to what a normal distribution density function looks like. On top of that, it reinforces the conclusions taken about box plots given the fact that for cluster 3 a very intense peak is observable for values around 50 kJ/mol which corresponds to the mean of the descriptor values present in cluster 3.

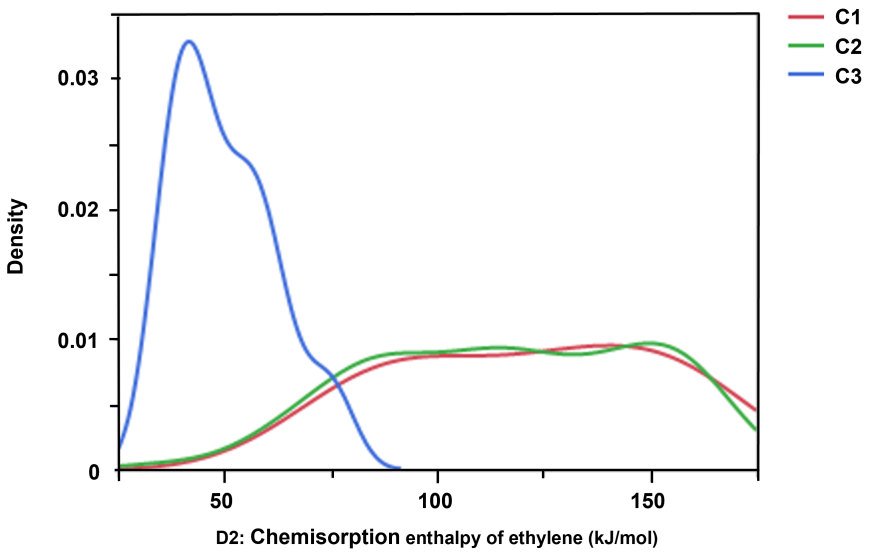

Figure 4.5: Comparison, in terms of probability density function, of the distribution for the chemisorption enthalpy of ethylene in all the three clusters.

Step 5-Building targeted libraries of virtual catalyst

Considering all the results obtained, a targeted library of virtual catalysts for each cluster will be created by applying the Chebyshev inequality, as in chapter 3, to the values taken into account for the chemisorption enthalpy of ethylene within each cluster. As stated before, by applying this principle we are certain that at least 50% of the virtual catalysts generated will be retained in a cluster.

Figure 4.6 and Figure 4.7 show the results obtained upon applying the targeting process to clusters 2 and 3, respectively. As expected, the shrinking of the descriptor ranges leads to a less broad range of performances, since the dots that represent virtual catalysts are closer to each other, but with a higher number of virtual catalysts per cluster, as stated on Table 4.7, approximating the distance between virtual and real catalysts performances. This was accomplished without an increase in the total number of virtual catalysts, which proves the targeting step was successful.

The trend obtained after the first iteration was retained after performing this step. Namely, cluster 2 is still characterized by catalysts with high conversion but lower selectivities, while cluster 3 contains catalysts with high conversions and high selectivities.

Table 4.7: Characteristics of the clusters obtained in the targeting step (step 5) for case study 1.

Descriptor	Number of virtual catalysts	$X_{Ethanol}$(%) (mean and standard deviation)	$S_{Ethylene}$(%) (mean and standard deviation)
Targeted C2	109	94.71 ± 8	1.90 ± 6
Targeted C3	105	96.47 ± 7	96.15 ± 6

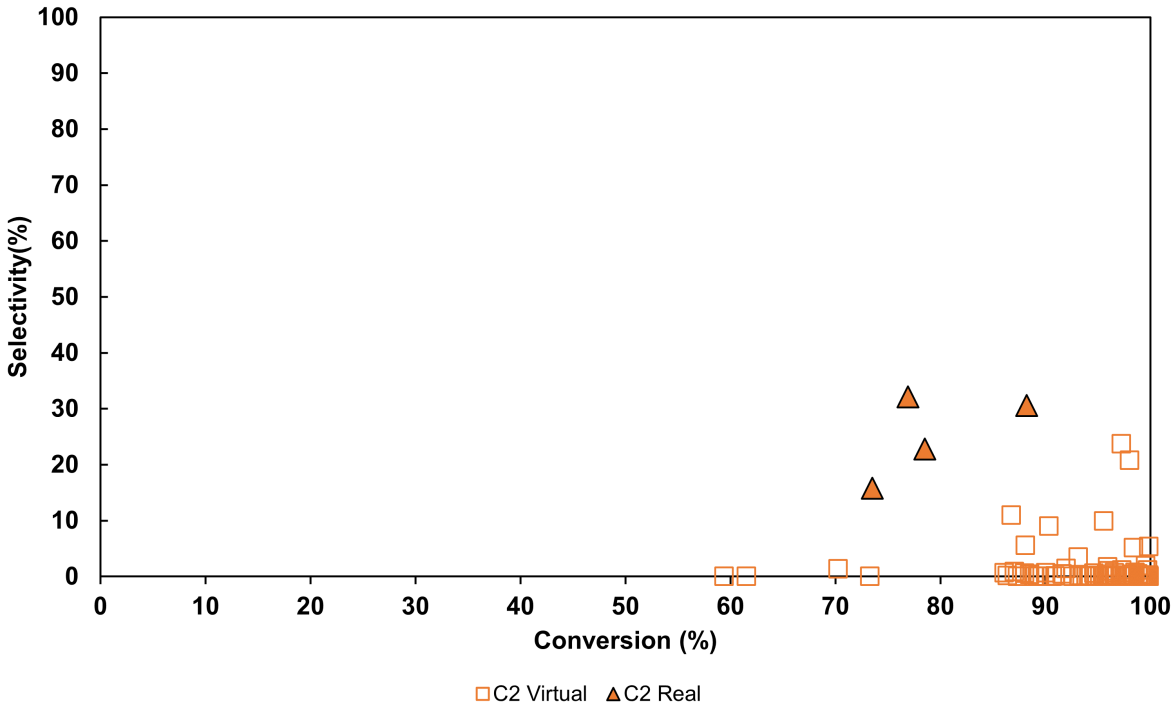

Figure 4.6: Result of the targeting step (step 5) for cluster 2 of case study 1.

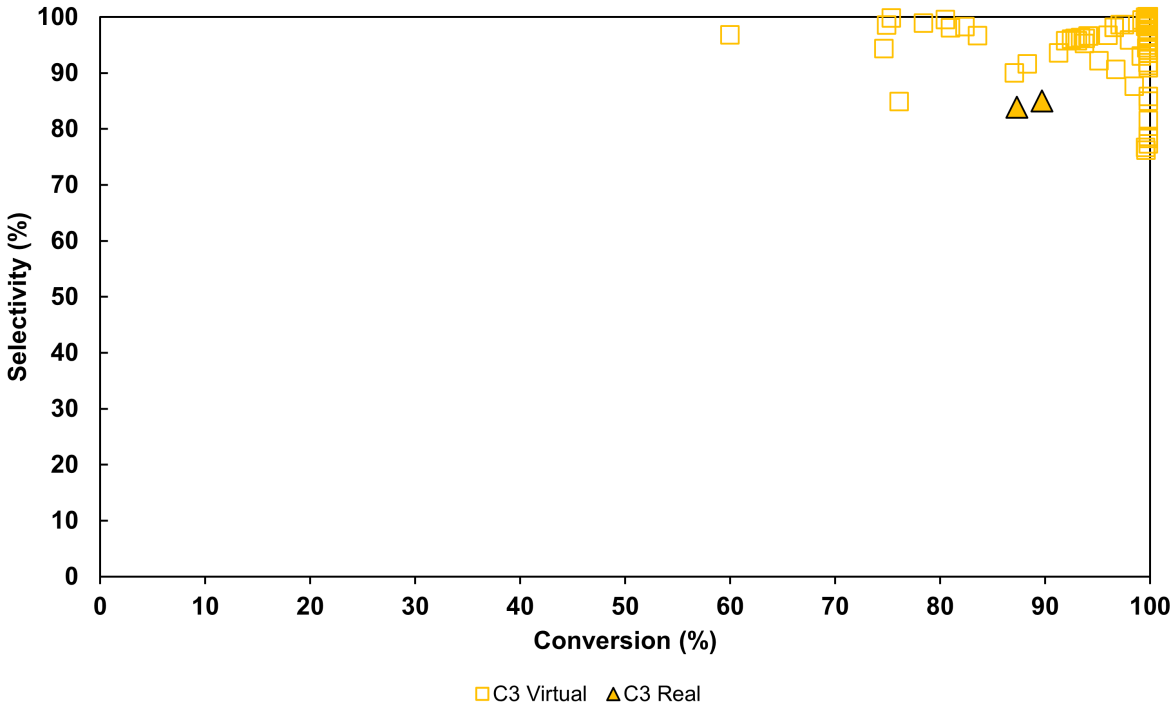

Figure 4.7: Result of the targeting step (step 5) for cluster 3 of case study 1.

Figure 4.8 represents the distribution of the identified relevant descriptor, explained previously, for the discovery library, the targeted library for cluster C2 and the targeted library for cluster C3. The presented descriptor ranges were the ones used to obtain Figure 4.6 and Figure 4.7, presented previously.

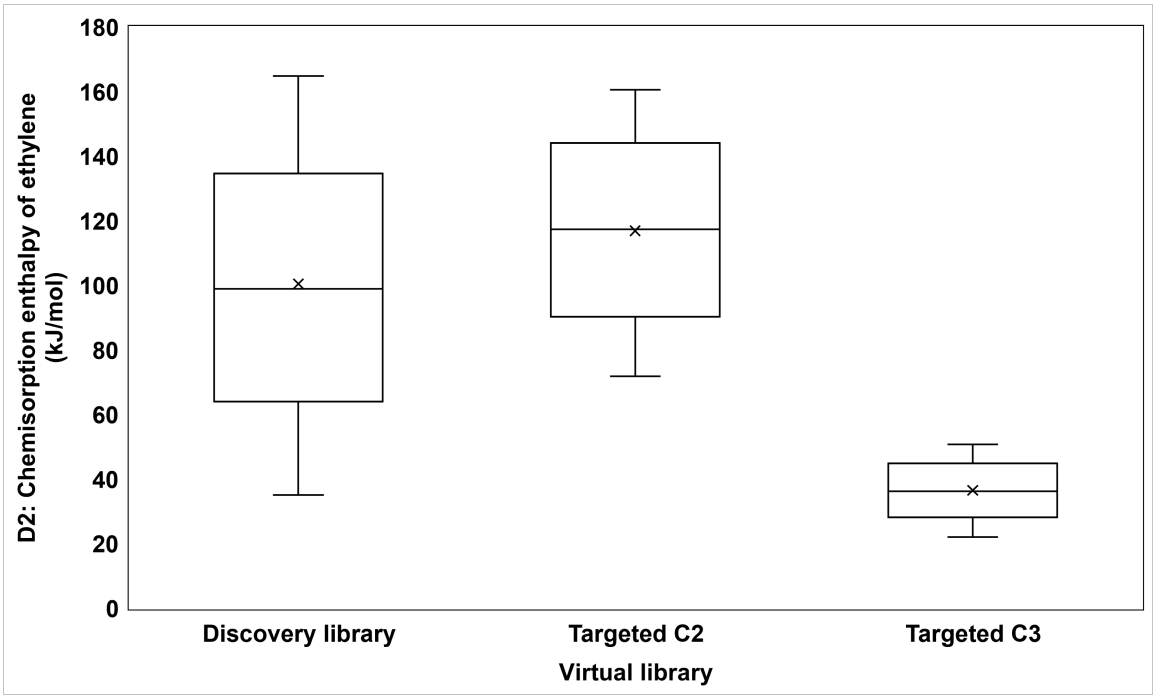

Figure 4.8: Comparison of the distribution of the relevant descriptor in the discovering and targeted libraries of virtual catalysts for case study 1.

Step 6 - Developing descriptor-property relationships from real catalysts properties

In order to relate catalyst compositions to these observations presented in Figure 4.8, a closer look at the catalyst characterization needs to be done. Looking at Table 4.4 it is possible to see that, as stated before, 6 different catalysts were studied being the BET surface one of the most pertinent studied characteristics for the studied dataset, given the fact that it is a relevant property for the chemisorption enthalpy as well. This has the objective of understanding the physical adsorption of gaseous species on solid materials and assumes that adsorption happens by multilayer creation and that there are an infinite number of layers being adsorbed at the saturation pressure, which means that the adsorption happens as if it was on a free surface [82].

The HZSM-5 catalyst that was modified by the addition of only phosphorous presents a very big performance drop, when compared to the unmodified HZSM-5 zeolite, especially in terms of selectivity. This can be due to a high reduction in the BET surface area of the catalyst, also to lower pore volume and width and, lastly, to a decrease in the total acidity amount of the catalyst as demonstrated in Table 4.4 and reported by N.Zhan *et al.* [24]. Considering that the density of active sites was not identified as a

relevant descriptor, this change in the total acidity could not be a major influence on the observed results, however, the p-value for the density of active sites was very close to the one taken into account as a threshold, so the acidity can end up being an impactful factor. This decrease in the total acidity amount is reported to have led to a major decrease in the quantity of stronger acid sites diminishing the acidic strength of the catalyst, which is a very important characteristic of the catalyst, and consequently hurting its performance given the fact that this process is usually catalyzed by strongly acidic zeolites [83].

On the other hand modification with lanthanum has enhanced catalyst performance at the studied operational conditions. This is probably associated with the increase in BET surface area and micropore volume, as stated on Table 4.4. Moreover, it is reported that adding lanthanum to HZSM-5 can improve the stability of the $[AlO_4]^-$ anion, which can be also one of the reasons why the HZSM-5 zeolite modified with just lanthanum is the one that presents a better performance out of all of the catalysts present in the dataset [84].

By analysing Figure 4.8 it is possible to observe that the targeted library for cluster 2, which is associated with lower selectivities for ethylene, reveals to have higher values for the ethylene chemisorption enthalpy when compared to the targeted library of cluster 3, related to a high selectivity for this compound that presents lower values for the ethylene chemisorption enthalpy.

So, taking into account these considerations on catalyst characteristics and the shown relations in Figure 4.8, one can conclude that higher values of the chemisorption enthalpy of ethylene are directly correlated to the presence of phosphorous, lower amounts of acidic strength of the catalyst and BET surface area, and consequently, to worst catalytic performance.

4.3.2 Case Study 2

Another set of experimental data was taken from Ref [3], where zeolites have been dealuminated apart from being only doped with metals, as it was the case in Case study 1. In this study, six different ZSM-5 zeolites were prepared, characterized, and tested, differing in the doping metal or the degree of dealumination. These catalysts are listed in Table 4.8 accompanied by corresponding conversions and selectivities. Extension ”deAl” in the catalyst label is used to refer to the dealuminated catalysts, while the extension P and La indicates doping with phosphorous and lanthanum in the same order. The dealumination degree was 25,50 and 100% of the volume of oxalic acid used for catalyst preparation. Table 4.8 provides a summary of the main physical characteristics of the used catalyst in Case study 2.

Table 4.8: Real catalysts and respective performances for dataset 2 [3].

Catalyst	$X_{ethanol}$(%)	$Y_{ethylene}$(%)	$S_{ethylene}$(%)
ZSM-5	45.8	3.98	6.11
ZSM-5 deAl-1/25	96.3	94.5	100
ZSM-5 deAl-1/50	82.5	30.1	33.4
ZSM-5 deAl-1/100	85.3	29.9	35.9
ZSM-5-P	41.8	9.97	23.8
ZSM-5-La	41.8	7.77	25.3

Reaction condition:0.4g of catalyst, atmospheric pressure, WHSV = $1.5h^{-1}$.

Table 4.9: Characteristics of the zeolites from the dataset 2 [3].

	Surface Area (m^2 g^{-1})			Pore volume (cm^3 g^{-1})	
Catalyst	SBET	Smicro	Sext	Vmicro	Vmeso
ZSM-5	372	245	127	0.13	0.13
ZSM-5 deAl-1/25	401	206	195	0.11	0.16
ZSM-5 deAl-1/50	447	214	232	0.12	0.19
ZSM-5-P	386	191	195	0.11	0.16
ZSM-5-La	381	194	186	0.11	0.15

Step 2-Numerical experiments

Similarly to the previously presented case study, the virtual catalysts performances were simulated with the developed microkinetic model, by making use of the same discovery library as in Case study 1 generated in section 4.1 and presented in Table A.1 of appendix A, and the obtained results are presented in Figure 4.9.

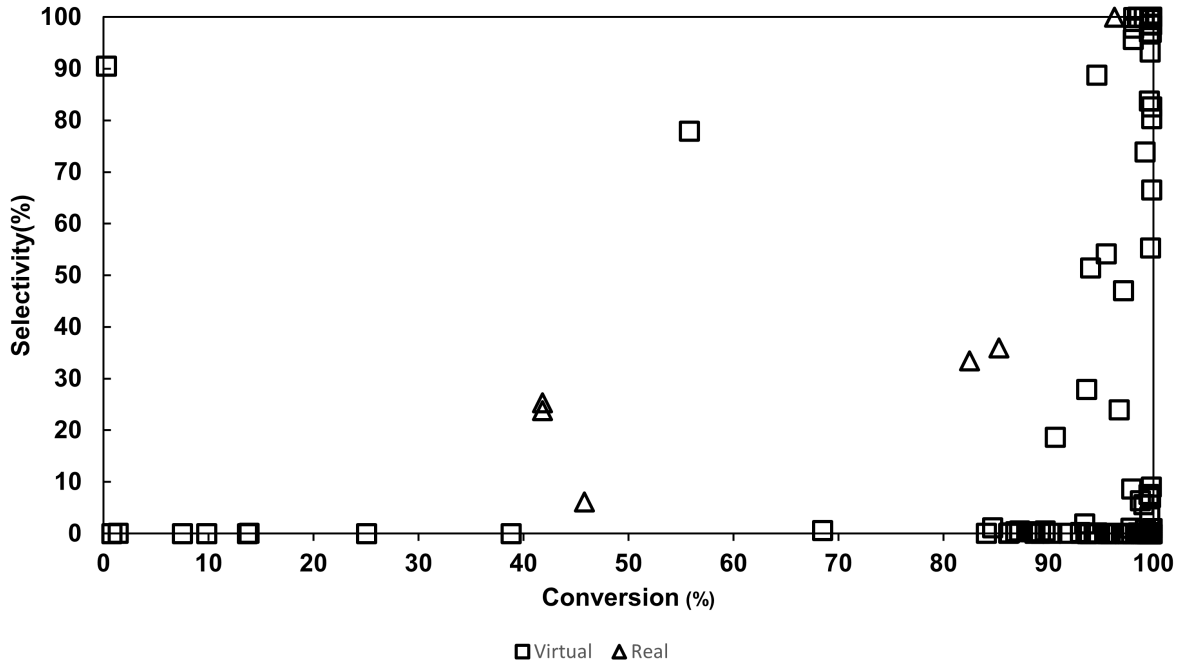

Figure 4.9: Obtained performances for the simulated virtual catalysts and the respective real catalysts from the dataset 2.Reaction conditions:T=493K, W=0.4g of catalyst, atmospheric pressure, WHSV = 1.5h^{-1}.

Step 3- Comparison between the performances of virtual and real catalysts

Three different clusters were also identified, in this case, by applying the silhouette method in the software *Orange3*. All three clusters contain virtual and real catalysts. In analogy to the previous case study, these three clusters are marked in blue, orange and yellow corresponding, respectively, to lower conversions and selectivities, with high conversion but low selectivity and high conversion and selectivities.

Table 4.10 provides a brief summary on each cluster characteristics, while Figure 4.10 visualizes the results of the clustering step after this first iteration of the methodology.

Table 4.10: Description of the three obtained clusters by application of k-means clustering technique to the 2nd dataset.

Cluster	Colour	Number of real catalysts	Number of virtual catalysts	$X_{Ethanol}$(%) (mean and standard deviation)	$S_{Ethylene}$(%) (mean and standard deviation)
C1	Blue	3	9	20.06 $\pm$18	12.15$\pm$26
C2	Orange	2	80	95.68$\pm$6	2.40$\pm$7
C3	Yellow	1	31	97.46$\pm$5	88.69$\pm$29

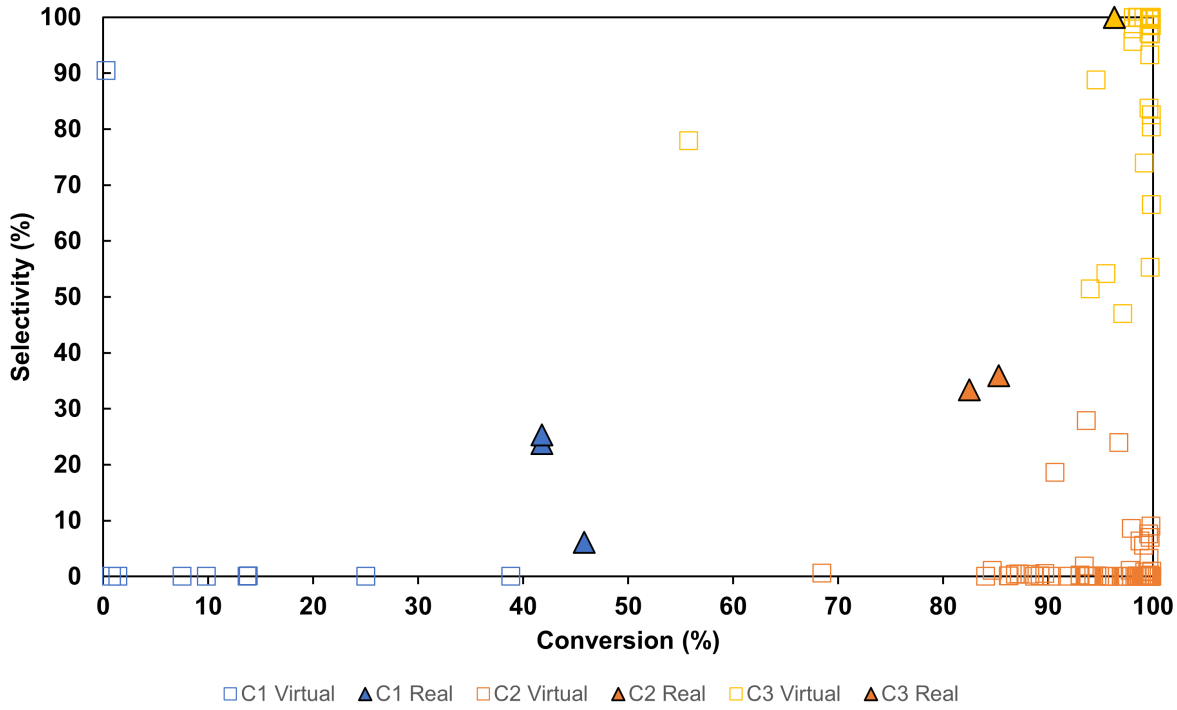

Figure 4.10: Output of the clustering step performed in *Orange3* for the 2nd dataset.

Step 4- Statistical analysis of the descriptor distributions

Having applied the statistical tests, which this time was the Kruskal Wallis test, due to having more than two clusters with real catalysts, it was possible to identify the discriminating descriptors for this case.

The same threshold of 0.05 was applied as the boundary for the p-value to filter more from less influential descriptors, which were the chemisorption enthalpies of ethanol, ethylene and DEE, as summarized in Table 4.11.

Table 4.11: Results of the statistical tests applied to each descriptor

Descriptor	p-value
$\Delta H_{chemisorption,Ethanol}$	<0.001
Δ $H_{chemisorption,Ethylene}$	<0.001
$\Delta H_{chemisorption,DEE}$	0.02
$S_{0,Ethanol}$	0.66
$S_{0,Ethylene}$	0.29
$\rho_{active\ sites}$	0.36

Figure 4.11, Figure 4.12 and Figure 4.13 show the comparison of the obtained distributions for the three relevant descriptors in the three clusters. Once again it is possible to observe that the descriptors do not follow a normal distribution and that, like in the first case study, there are already some trends that

can be verified especially for the first two descriptors. Namely cluster 1 which presents very low values for ethanol chemisorption enthalpy, also cluster 3 presents very low values for ethylene chemisorption enthalpy, similarly to Case study 1. Cluster 1 presents an outlier, which is the numeric point, represented by a dot, that is outside the box plot. This point is named an outlier because it is numerically far from the remainder of the data [85].

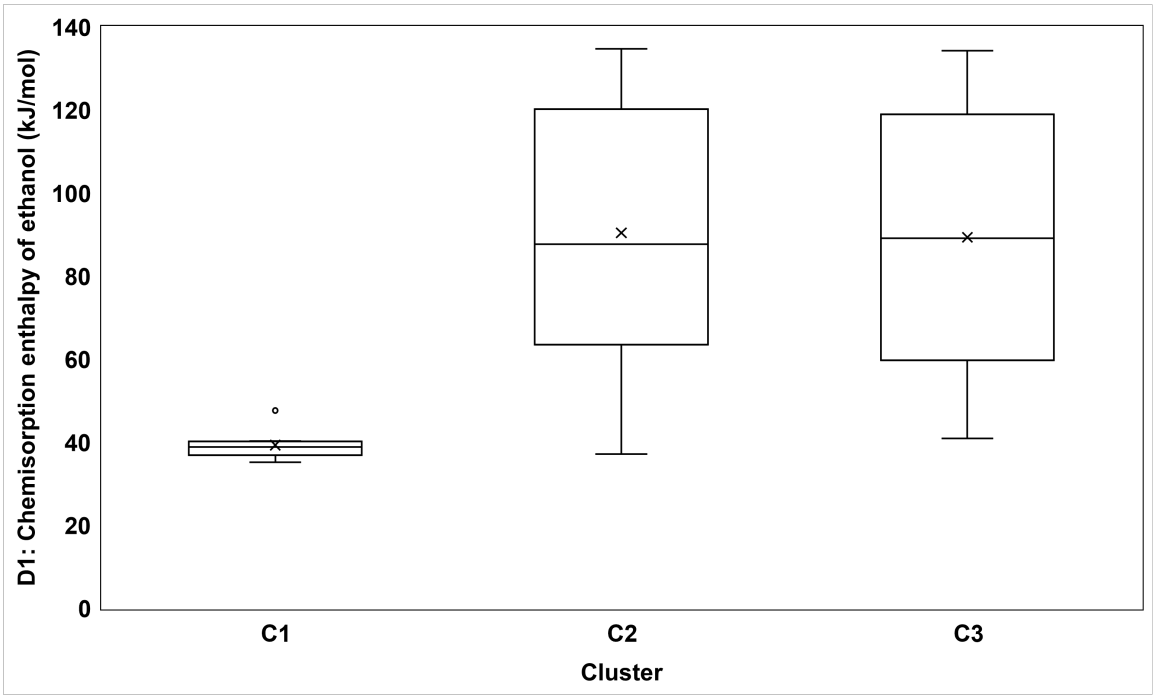

Figure 4.11: Comparison of the distributions of the chemisorption enthalpy of ethanol between clusters for the discovery library of case study 2.

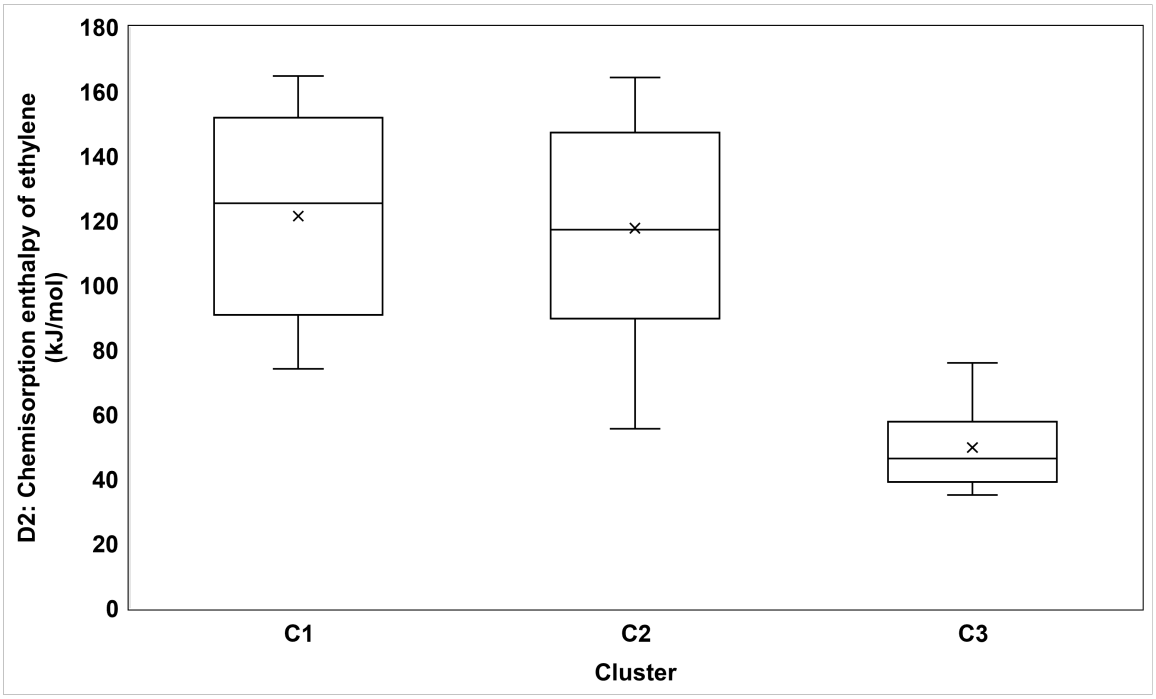

Figure 4.12: Comparison of the distributions of the chemisorption enthalpy of ethylene between clusters for the discovery library of case study 2.

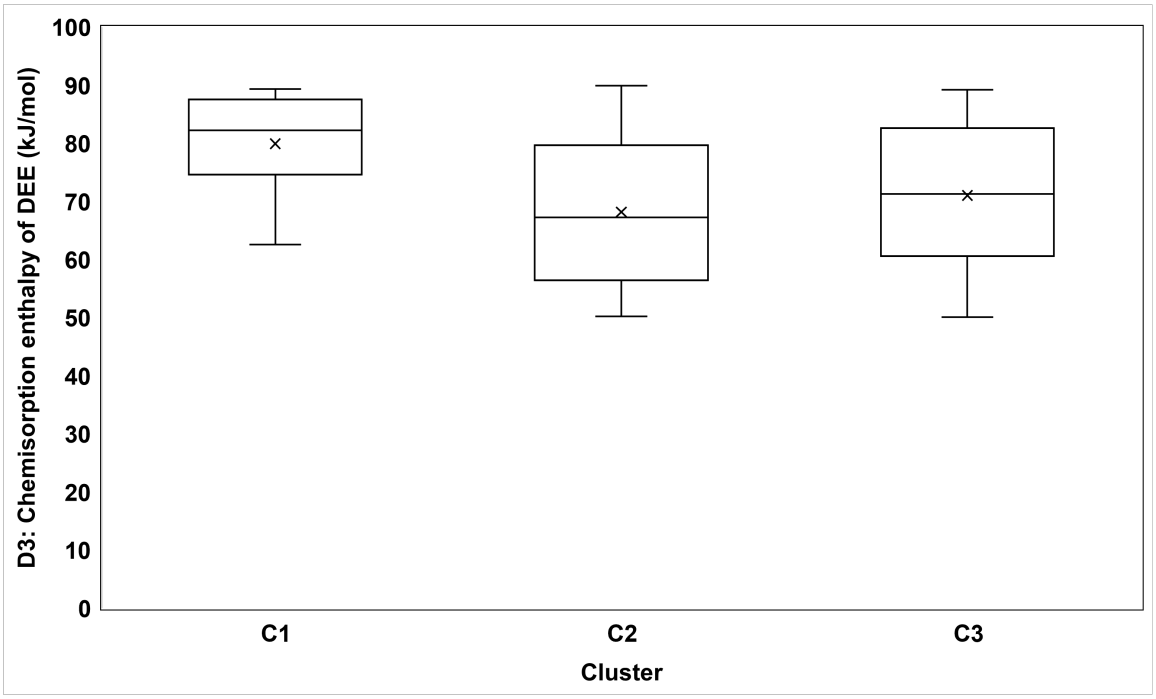

Figure 4.13: Comparison of the distributions of the chemisorption enthalpy of DEE between clusters for the discovery library of case study 2.

Step 5- Building targeted libraries of virtual catalysts

The Chebyshev inequality was again applied to the clusters obtained in step 4 by using virtual catalysts from the discovery library. In Figure 4.14 and Figure 4.15 the results obtained by the targeting process to clusters 1 and 2 are presented.

By visual intuition, one could say that the targeting process has been successful for both of the clusters, due to the fact that the number of virtual catalysts in the cluster is higher than that obtained for the discovery library. However, both of the clusters after the targeting step do not contain real catalysts anymore. This could be because the real catalysts for both of these clusters were close to their boundaries, representing one of the major downsides of using a dataset with low quantities of real catalysts($<$10 samples), as is the case.

Regarding cluster number three, one can say that the targeting step was developed with success. Not only the number of virtual catalysts was extended but also the real catalyst was retained within the cluster with virtual catalyst performances being closer to the real one, as can be seen on Figure 4.16.

A summary of the main features of this cluster is presented in Table 4.12, being characterized by high ethanol conversion and ethylene selectivity.

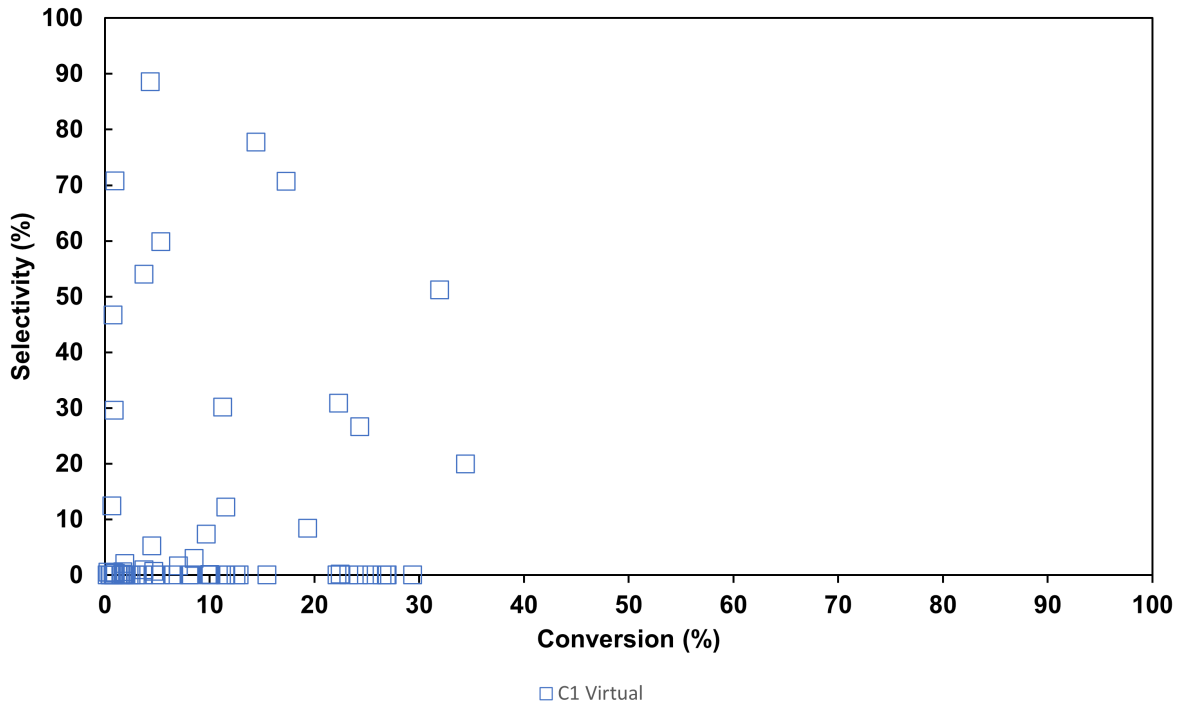

Figure 4.14: Result of the targeting step (step 5) for cluster 1 of case study 2.

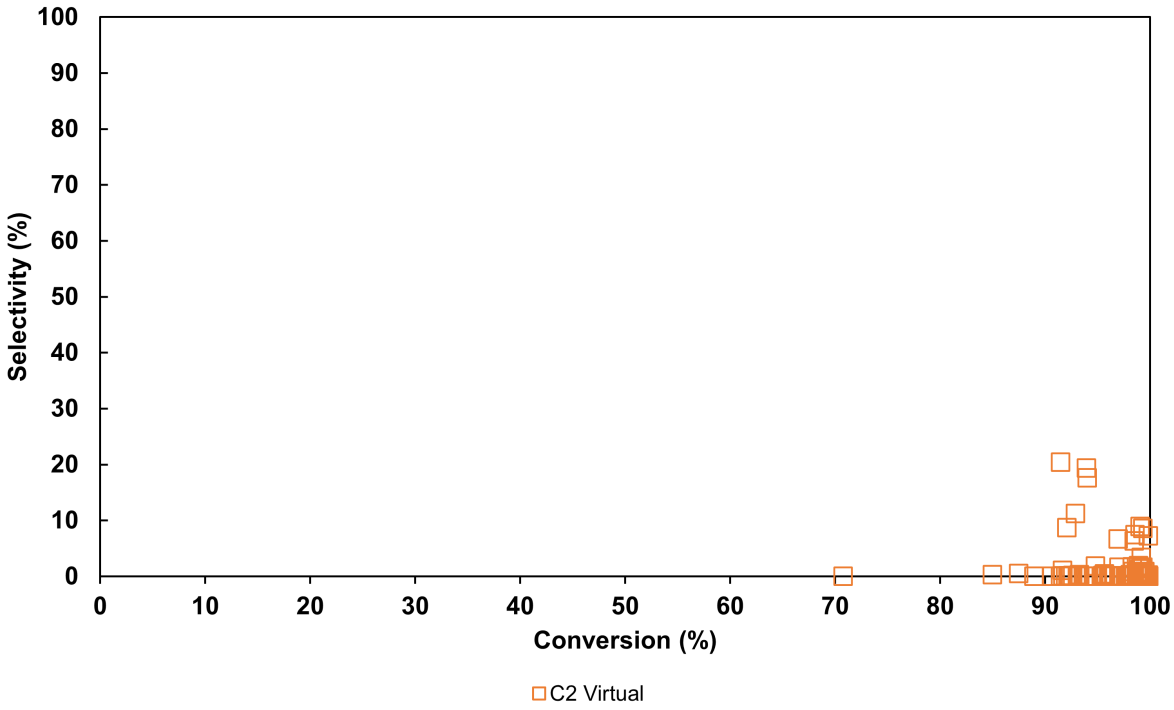

Figure 4.15: Result of the targeting step (step 5) for cluster 2 of case study 2.

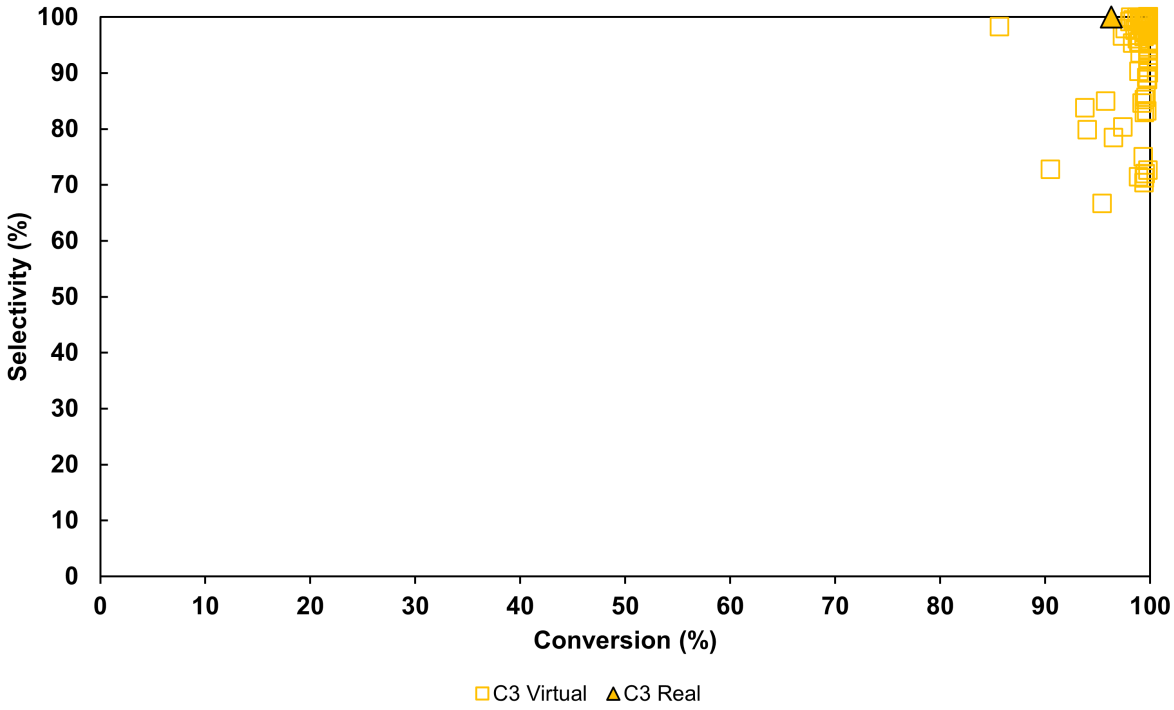

Figure 4.16: Result of the targeting step (step 5) for cluster 3 of case study 2.

Table 4.12: Characteristics of the clusters obtained in the targeting step (step 5) for case study 2.

Descriptor	Number of virtual catalysts	$X_{Ethanol}$(%) (mean and standard deviation)	$S_{Ethylene}$(%) (mean and standard deviation)
Targeted C2	97	99.02 ± 2	94.27 ± 9

Based on the results of this targeting step, it is possible to affirm that only cluster three can be considered relevant for further investigation. Hence, only the descriptor distributions for this cluster were further statistically studied and the obtained results are shown in Figure 4.17, Figure 4.18 and Figure 4.19 for the distribution of the three discriminating descriptors(the chemisorption enthalpies of ethanol, ethylene and DEE).

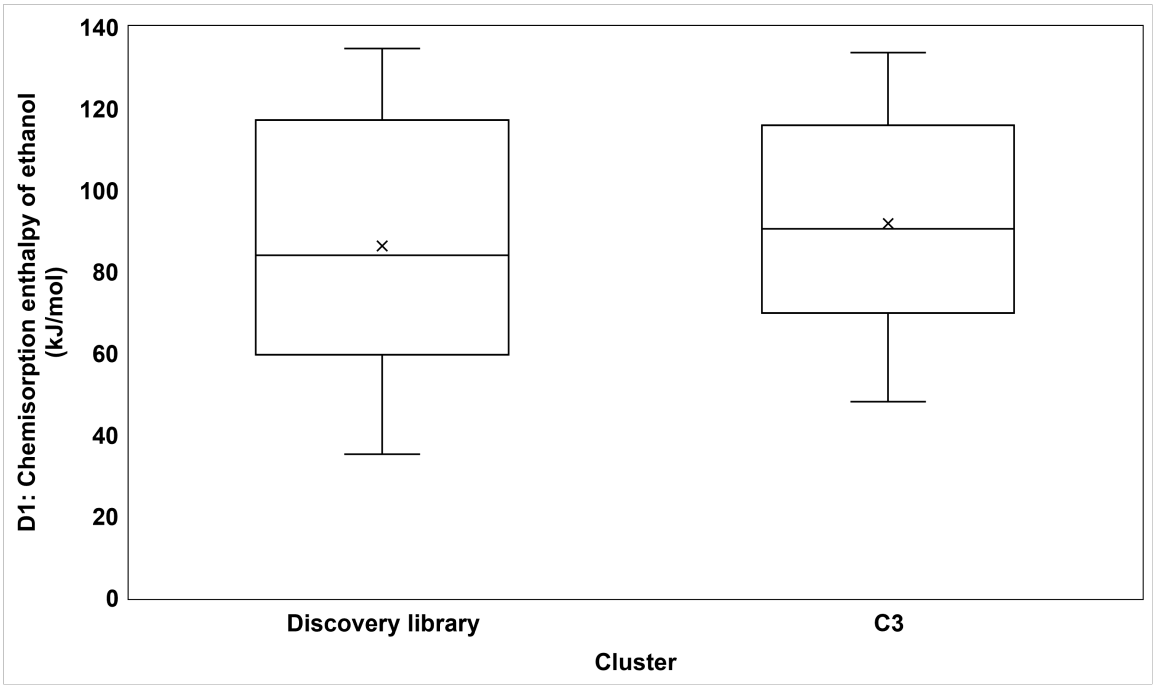

Figure 4.17: Comparison of the distributions of the chemisorption enthalpy of ethanol in the discovery library and target library of virtual catalysts for case study 2.

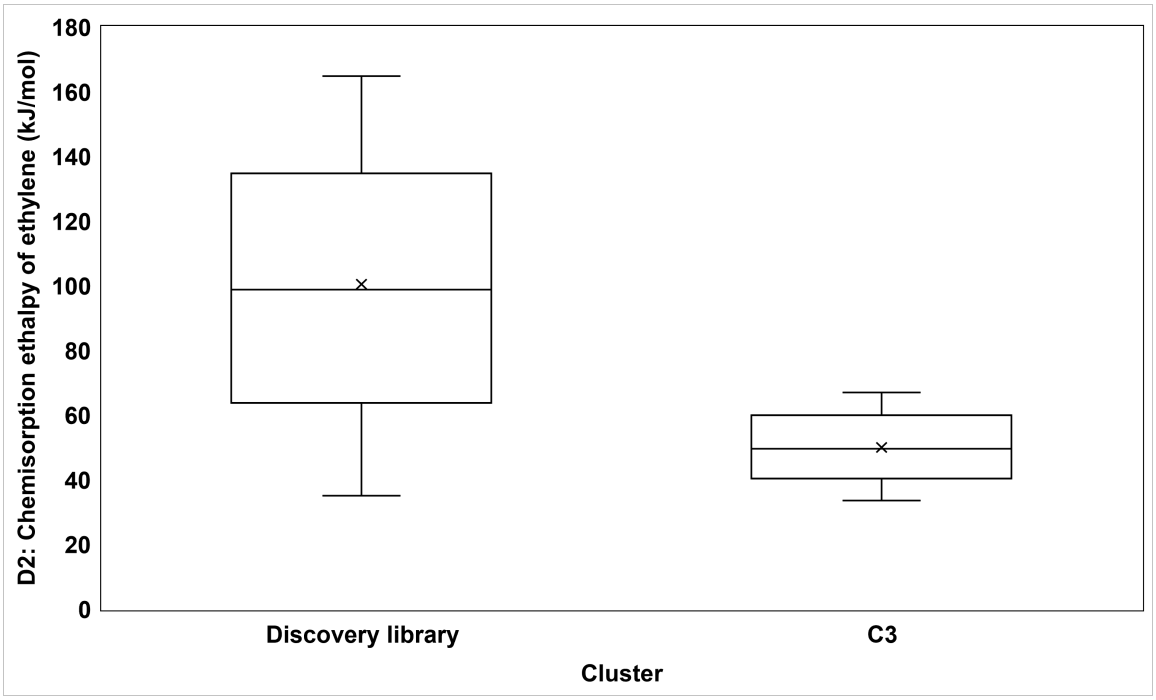

Figure 4.18: Comparison of the distributions of the chemisorption enthalpy of ethylene in the discovery library and target library of virtual catalysts for case study 2.

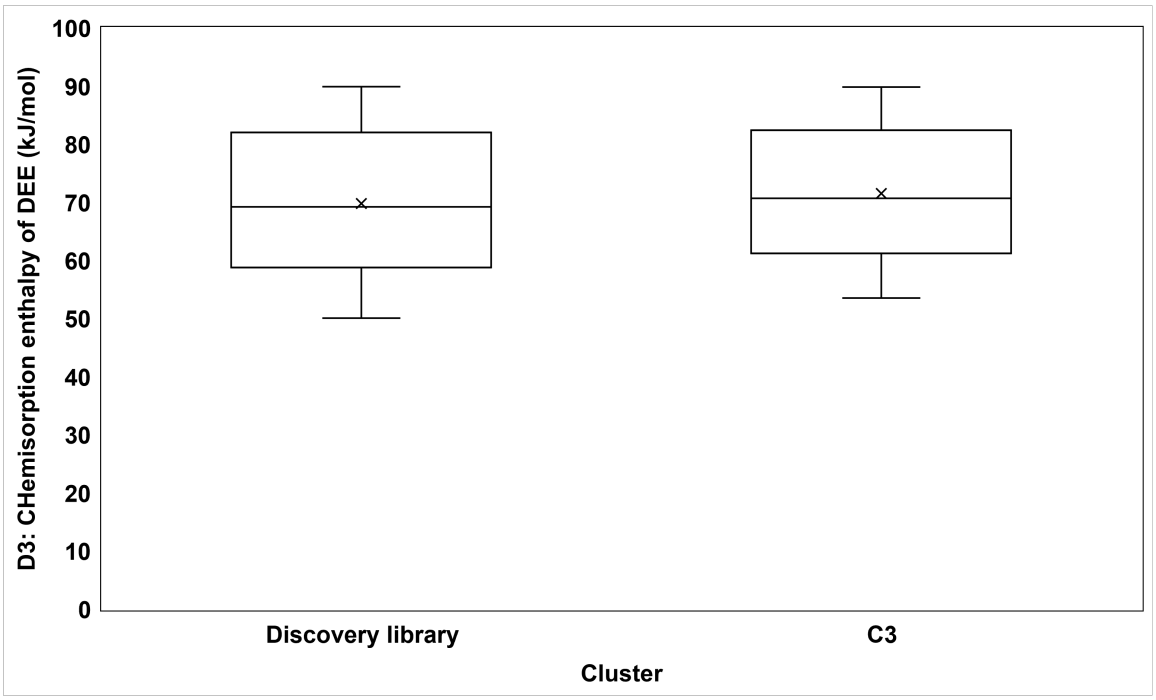

Figure 4.19: Comparison of the distributions of the chemisorption enthalpy of DEE in the discovery library and target library of virtual catalysts for case study 2.

Step 6- Developing descriptor-property relationships from real catalysts properties

Firstly, through analysis of the previously presented boxplots, the hypothesis from case study 1, of lower ethylene chemisorption enthalpies being related to better catalyst performance is corroborated by the study of the second dataset as can be proven by Figure 4.19. Moreover, since both ZSM-5 doped with phosphorous and lanthanum present poor performance on this dataset, the presence of synergy between these two when catalysts are doped with both can be a possibility, due to the observed data from case study 1 as already previously reported [24].

Concerning the chemisorption enthalpies of ethanol and DEE by taking a look at the distributions of these descriptors between the discovery library and the studied cluster, it is not possible to take any kind of conclusions, despite the fact they are statistically relevant. However, this reassures us that the chemisorption enthalpy of ethylene can be considered the most discriminating descriptor of the process in the simulated conditions.

In the case of the third cluster, the only real catalyst present is a dealuminated ZSM-5 zeolite, being the one where 25% of oxalic acid was used during catalyst preparation. Since only this sample is present in the cluster and, on top of that, cluster 2 also has ZSM-5 zeolites that have been dealuminated but with higher percentages of oxalic acid, the assumption that a dealumination step during the catalyst synthesis process could influence the identified relevant descriptors and, in this case, the selectivity for ethylene of the process cannot be statistically proven. Thus, it is not possible to establish any kind of relationship between catalyst characteristics and the observed performance.

5

Conclusions

Conclusions

The work developed in this thesis had the aim of allowing the design of new catalysts for ethanol dehydration to ethylene process, by trying to establish relations between physical properties and the verified performance, making use of a recently developed approach. This process is of major importance since it is seen as one of the biggest alternatives to the conventional routes for olefin production, especially when considering the need for this kind of chemical.

The used methodology consists of a comprehensive methodology denominated Model-driven catalyst design. This is performed with the help of several statistical tools and techniques namely the FFF design, k-means clustering, through *Orange3* software and the Mann-Whitney and Kruskal-Wallis tests, by making use of *JMP16* software. A fundamental microkinetic model is also needed to perform the simulations for different conditions and catalysts.

First of all, concerning the kinetic model development, this revealed to be hard to model due to numerical problems related to the very broad range of magnitude associated with the rate constants of the process. As a consequence, several different approaches needed to be considered and the usage of scaling factors was needed.

Secondly, regarding the followed catalyst design technique, as it was already proven in previous works [46], the application of the methodology itself can be considered as successful, representing an important tool in facing the biggest problems related to the kinetics-driven design of catalysts since it allows to create direct relations between the chemical properties and the results obtained on the statistical tests while being less expensive and time-consuming. Furthermore, even though it helps to have big sets of experimental data, it is proven by this work that it still works with smaller sets, being this a very promising feature to be taken into account for the future. However, some improvements still need to be made, especially in trying to use fewer tools so it is more integrated and efficient, as stated in [46].

When applied to ethanol dehydration to ethylene, for Case study 1, one can conclude that the chemisorption enthalpy of ethylene is the discriminating descriptor and that lower values for this are associated with better catalytic performance, while higher values for this are related to worse catalytic performance, especially in terms of selectivity. This is possibly connected to a reduction in the BET surface area and in the volume and width of the pores related to metal doping a catalyst, especially with phosphorous in this case. On top of this, a big decrease in the total acid amount, especially in the acidic strength of the catalysts, which constitutes an important property for the studied process, is verified for the catalyst associated with the worst performances. This conclusion is based on three different clusters that were obtained, having two both virtual and real catalysts. On the other hand, it was possible to infer that lower values of the ethylene chemisorption enthalpy are associated with higher ethanol conversion and selectivity for ethylene.

As for case study 2, the low number of real catalysts proved to be a setback for this study, leading

to a non-successful targeting step and a lack of statistically relevant results that didn't allow taking conclusions. Thus, even though, it is possible to perform the methodology and reach conclusions and results with samples containing lower amounts of real catalysts, it can be concluded that a big dataset should always be used to make sure that the methodology is always successful.

Overall, even though this constitutes a set of preliminary conclusions and more studies should be done to acquire more relationships and prove what was concluded until this point, the applicability of the methodology was successful with the chemisorption enthalpy of ethylene being discovered as the main factor influencing the performance of zeolites for the studies datasets. This appeared related to the acid strength of the catalyst and the surface area available for adsorption. Both of these properties can be manipulated by modifying catalyst structure mainly through metal doping processes and this should be taken into account for further studies, especially in design phases for real catalysts, so the ethanol dehydration process can overcome the issue associated with catalysts and reach its full potential in order to aid the environmental change that is needed nowadays.

6

Future work

Future work

First of all, the main focus of future works that might be done on this application is regarding the kinetic model developed for the application of the methodology. Given the fact that high numerical problems were encountered, new approaches for the model development and more research to check if the model works according to reality should be done especially considering the importance that this can have on the observed results.

Secondly, the number of descriptors used or the number of steps where they are implemented can also be a subject of change in the future. Even though these have only been applied to adsorption and desorption steps in the present work, there are already some works regarding this procedure that apply them in other kinds of steps [64].

For that, they make use of the Brönsted- Evans-Polanyi principle. This principle defends that there is a proportional relationship between the difference in the activation energies of two reactions of the same family and their reaction enthalpies, as stated by eq. (6.1) [86, 87], where Ea is the activation energy of a reaction from the same family, ΔH is the enthalpy of the reaction that is being studied and α is the transfer coefficient of the Polanyi-relationship.

$$Ea = E_0 + \alpha \Delta H \tag{6.1}$$

The descriptor, in this case, would be implemented via the enthalpy of the reaction term, as reported by J. Sun *et al* [64]. However, the amount of data regarding the values of the needed parameters for the application of this equation is still scarce, especially when considering the set of reactions in this study. So a study of it could be helpful to improve the quality of the obtained results and assess the effect of more catalyst characteristics.

Regarding the methodology itself, there is still plenty of room to improve it. So for future work, the methodology should be applied to many more datasets with different catalyst modifications and compositions to be able to establish improved relationships between performance and properties. Another thing that could help would be creating a broader dataset with many more studied real catalysts, so more clusters with real and virtual catalysts would be obtained and then more conclusions could be taken. Additionally, an optimization step could be added to the methodology. This could be done, for example, by applying regression to the obtained libraries and respective intervals of values, so numeric correlations can be obtained, and better assumptions can be made on a consequent design phase.

Lastly, as suggested in previous works [46], integrating all the steps into just one tool is also a task to make the procedure more efficient. For example, this can be achieved by using *Python* or Matlab software and its packages.

Bibliography

[1] H. Rahmanifard, N. Experience, S. Alpha, and K. Mascarenhas, "Economic impacts and market challenges for the methane to derivatives petrochemical sub-sector," March 2018.

[2] I. Amghizar, L. A. Vandewalle, K. M. V. Geem, and G. B. Marin, "New trends in olefin production," *Engineering*, vol. 3, pp. 171–178, April 2017.

[3] C.-Y. Wu and H.-S. Wu, "Ethylene formation from ethanol dehydration using zsm-5 catalyst," *ACS Omega*, vol. 2, no. 8, pp. 4287–4296, 2017, pMID: 31457720.

[4] K. V. der Borght, K. Toch, V. V. Galvita, J. W. Thybaut, and G. B. Marin, "Information-driven catalyst design based on high-throughput intrinsic kinetics," *Catalysts*, vol. 5, pp. 1948–1968, November 2015.

[5] H. Zimmermann and R. Walzl, *Ullmann's Encyclopedia of Industrial Chemistry*. Wiley-VCH Verlag GmbH & Co. KGaA, April 2009, vol. 13.

[6] H. Al-Megren and T. Xiao, *Petrochemical catalyst materials, processes, and emerging technologies*. IGI Global, 2016.

[7] A. Editors, *Ethylene from bioethanol*. McGraw-Hill Education, September 2014.

[8] M. Zhang and Y. Yu, "Dehydration of ethanol to ethylene," *Industrial and Engineering Chemistry Research*, vol. 52, pp. 9505–9514, July 2013.

[9] C. Corporation. (2017) Ethylene derivatives. Accessed on 25/03/2022. [Online]. Available: https://www.chiyodacorp.com/en/service/chemistry/ethylene/

[10] A. Mohsenzadeh, A. Zamani, and M. J. Taherzadeh, "Bioethylene production from ethanol: A review and techno-economical evaluation," *ChemBioEng Reviews*, vol. 4, pp. 75–91, April 2017.

[11] Batchu, Rakesh, "Bioethanol conversion to hydrocarbons : role of products and intermediates," Ph.D. dissertation, Ghent University, 2017.

[12] T. J. Tse, D. J. Wiens, and M. J. T. Reaney, “Production of bioethanol—a review of factors affecting ethanol yield,” *Fermentation*, vol. 7, no. 4, 2021.

[13] H. Aditiya, T. Mahlia, W. Chong, H. Nur, and A. Sebayang, “Second generation bioethanol production: A critical review,” *Renewable and Sustainable Energy Reviews*, vol. 66, pp. 631–653, 2016.

[14] M. Sillanpää and C. Ncibi, *A Sustainable Bioeconomy: The Green Industrial Revolution*. Springer International Publishing, 2017.

[15] Y. Lin and S. Tanaka, “Ethanol fermentation from biomass resources: Current state and prospects,” *Applied Microbiology and Biotechnology*, vol. 69, pp. 627–642, February 2006.

[16] A. Bušić, N. Mardetko, S. Kundas, G. Morzak, H. Belskaya, M. I. Santek, D. Komes, S. Novak, and B. Šantek, “Bioethanol production from renewable raw materials and its separation and purification: A review,” *Food Technology and Biotechnology*, vol. 56, September 2018.

[17] R. E. Kirk, D. F. Othmer, M. Grayson, and D. Eckroth, *Kirk-Othmer Encyclopedia of chemical technology*, 2000, pp. 593–632.

[18] D. W. Posch, “Polyolefins,” *Applied Plastics Engineering Handbook: Processing, Materials, and Applications: Second Edition*, pp. 27–52, September 2016.

[19] I. Amghizar, J. Dedeyne, D. Brown, G. Marin, and K. Van Geem, “Sustainable innovations in steam cracking: Co2 neutral olefin production,” *Reaction Chemistry & Engineering*, vol. 5, February 2020.

[20] T. Ren, M. K. Patel, and K. Blok, “Steam cracking and methane to olefins: Energy use, co2 emissions and production costs,” *Energy*, vol. 33, pp. 817–833, 2008.

[21] D. Fan, D. J. Dai, and H. S. Wu, “Ethylene formation by catalytic dehydration of ethanol with industrial considerations,” pp. 101–115, 2013.

[22] M. F. Reyniers and G. B. Marin, “Experimental and theoretical methods in kinetic studies of heterogeneously catalyzed reactions,” *Annual Review of Chemical and Biomolecular Engineering*, vol. 5, pp. 563–594, 2014.

[23] J. Moulijn, M. Makee, and A. E. V. Diepen, *Chemical Process Technology*, 2nd ed. Wiley, 2013, vol. 2.

[24] N. Zhan, Y. Hu, H. Li, D. Yu, Y. Han, and H. Huang, “Lanthanum–phosphorous modified hzsm-5 catalysts in dehydration of ethanol to ethylene: A comparative analysis,” *Catalysis Communications*, vol. 11, no. 7, pp. 633–637, 2010.

[25] K. V. der Borght, “Omzetting van bio-ethanol naar koolwaterstoffen: van laboratorium tot industriële schaal,” Ph.D. dissertation, Universiteit Ghent, 2015.

[26] M. N. Timofeeva, “Acid catalysis by heteropoly acids,” *Applied Catalysis A: General*, vol. 256, pp. 19–35, December 2003.

[27] S. Yu, X. Zhao, G. Su, Y. Wang, Z. Wang, K. Han, and H. Zhu, “Synthesis and electrocatalytic performance of a p-mo-v keggin heteropolyacid modified ag@pt/mwcnts catalyst for oxygen reduction in proton exchange membrane fuel cell,” *Ionics*, vol. 25, pp. 5141–5152, November 2019.

[28] K. Tanabe and W. F. Hölderich, “Industrial application of solid acid–base catalysts,” *Applied Catalysis A: General*, vol. 181, no. 2, pp. 399–434, 1999.

[29] J. Weitkamp, “Zeolites and catalysis,” *Solid State Ionics*, vol. 131, pp. 175–188, June 2000.

[30] B. Smit and T. L. Maesen, “Towards a molecular understanding of shape selectivity,” *Nature*, vol. 451, pp. 671–678, February 2008.

[31] G. Ertl, H. Knözinger, and J. Weitkamp, Eds., *Handbook of Heterogeneous Catalysis*. Wiley, July 1997, vol. 5.

[32] V. Mouarrawis, R. Plessius, J. I. van der Vlugt, and J. N. H. Reek, “Confinement effects in catalysis using well-defined materials and cages,” *Frontiers in Chemistry*, vol. 6, 2018.

[33] A. Feliczak-Guzik, “Hierarchical zeolites: Synthesis and catalytic properties,” *Microporous and Mesoporous Materials*, vol. 259, pp. 33–45, 2018.

[34] L.-H. Chen, M.-H. Sun, Z. Wang, W. Yang, Z. Xie, and B.-L. Su, “Hierarchically structured zeolites: From design to application,” *Chemical Reviews*, vol. 120, pp. 11 194–11 294, 2020, pMID: 32915551.

[35] R. Gounder, “Hydrophobic microporous and mesoporous oxides as brønsted and lewis acid catalysts for biomass conversion in liquid water,” *Catal. Sci. Technol.*, vol. 4, pp. 2877–2886, 2014.

[36] G. Özçakır and A. Karaduman, “Effect of metal doped zsm-5 catalyst on aromatic yield and coke formation in microalgal bio-oil production,” *International Journal of Natural and Applied Sciences*, vol. 4, pp. 20–32, 2021.

[37] T. F. Robin, A. B. Ross, A. R. Lea-Langton, and J. M. Jones, “Stability and activity of doped transition metal zeolites in the hydrothermal processing,” *Frontiers in Energy Research*, vol. 3, 2015.

[38] Y. Fang, H. Zhang, X. Li, H. Huang, H. Xin, M. Lu, M. Li, and X. Li, “Ethylene production from ethanol over metal/phosphorus-modified zsm-5 catalysts,” *Energy and Environment Focus*, vol. 3, pp. 227–235, July 2014.

[39] K. Alexopoulos, M. John, K. V. D. Borght, V. Galvita, M. F. Reyniers, and G. B. Marin, "Dft-based microkinetic modeling of ethanol dehydration in h-zsm-5," *Journal of Catalysis*, vol. 339, pp. 173–185, July 2016.

[40] R. Batchu, V. V. Galvita, K. Alexopoulos, T. S. Glazneva, H. Poelman, M. F. Reyniers, and G. B. Marin, "Ethanol dehydration pathways in h-zsm-5: Insights from temporal analysis of products," *Catalysis Today*, vol. 355, pp. 822–831, September 2020.

[41] W. Wang, Y. Jiang, and M. Hunger, "Mechanistic investigations of the methanol-to-olefin (mto) process on acidic zeolite catalysts by in situ solid-state nmr spectroscopy," vol. 113, March 2006, pp. 102–114.

[42] S. Mehariya, A. Iovine, P. Casella, D. Musmarra, A. Figoli, T. Marino, N. Sharma, and A. Molino, "Chapter 7 - fischer–tropsch synthesis of syngas to liquid hydrocarbons," in *Lignocellulosic Biomass to Liquid Biofuels*, A. Yousuf, D. Pirozzi, and F. Sannino, Eds. Academic Press, 2020, pp. 217–248.

[43] J. J. H. B. Sattler, I. D. Gonzalez-Jimenez, L. Luo, B. A. Stears, A. Malek, D. G. Barton, B. A. Kilos, M. P. Kaminsky, T. W. G. M. Verhoeven, E. J. Koers, M. Baldus, and B. M. Weckhuysen, "Platinum-promoted ga/al2o3 as highly active, selective, and stable catalyst for the dehydrogenation of propane," *Angewandte Chemie International Edition*, vol. 53, no. 35, pp. 9251–9256, 2014.

[44] J. G. D. Vries and S. D. Jackson, "Homogeneous and heterogeneous catalysis in industry," *Catalysis Science and Technology*, vol. 2, p. 2009, October 2012.

[45] J. K. Nørskov and T. Bligaard, "The catalyst genome," *Angewandte Chemie International Edition*, vol. 52, pp. 776–777, January 2013.

[46] L. Pirro, P. S. Mendes, S. Paret, B. D. Vandegehuchte, G. B. Marin, and J. W. Thybaut, "Descriptor-property relationships in heterogeneous catalysis: Exploiting synergies between statistics and fundamental kinetic modelling," *Catalysis Science and Technology*, vol. 9, pp. 3109–3125, 2019.

[47] R. Tesser and V. Russo, *Advanced reactor modeling with MATLAB: Case studies with solved examples*. De Gruyter, December 2020.

[48] A. Chakkingal, L. Pirro, A. R. C. da Cruz, A. J. Barrios, M. Virginie, A. Y. Khodakov, and J. W. Thybaut, "Unravelling the influence of catalyst properties on light olefin production via fischer–tropsch synthesis: A descriptor space investigation using single-event microkinetics," *Chemical Engineering Journal*, vol. 419, September 2021.

[49] R. Lekivetz and B. Jones, "Fast flexible space-filling designs for nonrectangular regions," *Quality and Reliability Engineering International*, vol. 31, pp. 829–837, July 2015.

[50] Statistical software — jmp. Accessed on 11/05/2022. [Online]. Available: https://www.jmp.com/en_be/home.html

[51] Understanding k-means clustering in machine learning — by dr.michael j.garbade — towards data science. Accessed on 10/05/2022. [Online]. Available: https://towardsdatascience.com/understanding-k-means-clustering-in-machine-learning-6a6e67336aa1

[52] N. Sharma, "K-means clustering explained - neptune.ai," November 2021, accessed on 20/06/2022. [Online]. Available: https://neptune.ai/blog/k-means-clustering

[53] P. Patil, "K means clustering : Identifying f.r.i.e.n.d.s in the world of strangers — by prasad patil — towards data science," May 2018, accessed on 20/06/2022. [Online]. Available: https://towardsdatascience.com/k-means-clustering-identifying-f-r-i-e-n-d-s-in-the-world-of-strangers-695537505d

[54] Orange data mining - data mining. Accessed on 11/05/2022. [Online]. Available: https://orangedatamining.com/

[55] P. J. Rousseeuw, "Silhouettes: A graphical aid to the interpretation and validation of cluster analysis," *Journal of Computational and Applied Mathematics*, vol. 20, pp. 53–65, November 1987.

[56] D. Arthur and S. Vassilvitskii, "K-means++: The advantages of careful seeding," in *Proceedings of the Eighteenth Annual ACM-SIAM Symposium on Discrete Algorithms*, ser. SODA '07. USA: Society for Industrial and Applied Mathematics, 2007, p. 1027–1035.

[57] F. Wang, H.-H. Franco-Penya, J. D. Kelleher, J. Pugh, and R. Ross, "An analysis of the application of simplified silhouette to the evaluation of k-means clustering validity," in *Machine Learning and Data Mining in Pattern Recognition*, P. Perner, Ed. Cham: Springer International Publishing, 2017, pp. 291–305.

[58] Kruskal-wallis test: Definition, formula, and example - statology. Accessed on 11/05/2022. [Online]. Available: https://www.statology.org/kruskal-wallis-test/

[59] Mann whitney u test: Definition, how to run in spss - statistics how to. Accessed on 11/05/2022. [Online]. Available: https://www.statisticshowto.com/mann-whitney-u-test/#definition

[60] How to interpret a p-value less than 0.05 (with examples). Accessed on 4/10/2022. [Online]. Available: https://www.statology.org/p-value-less-than-0-05/

[61] C. Andrade, "The P value and statistical significance: Misunderstandings, explanations, challenges, and alternatives," *Indian J. Psychol. Med.*, vol. 41, no. 3, pp. 210–215, May 2019.

[62] Chebyshev's theorem in statistics - statistics by jim. Accessed on 11/05/2022. [Online]. Available: https://statisticsbyjim.com/basics/chebyshevs-theorem-in-statistics/

[63] Statistics how to. Accessed on 29/09/2022. [Online]. Available: https://www.statisticshowto.com/

[64] J. Sun, J. W. Thybaut, and G. B. Marin, "Microkinetics of methane oxidative coupling," *Catalysis Today*, vol. 137, no. 1, pp. 90–102, 2008, recent Developments in Combinatorial Catalysis Research and High-Throughput Technologies.

[65] Sticking probability. Accessed on 08/06/2022. [Online]. Available: https://www.chemeurope.com/en/encyclopedia/Sticking_probability.html

[66] C. chau Chiu, G. N. Vayssilov, A. Genest, A. Borgna, and N. Rösch, "Predicting adsorption enthalpies on silicalite and hzsm-5: A benchmark study on dft strategies addressing dispersion interactions," *Journal of Computational Chemistry*, vol. 35, pp. 809–819, April 2014.

[67] K. S. Abdulazizovna, Y. Y. Yusupboyevich, A. T. Dolimjonovich, and R. L. Sobirjonovna, "Adsorption energetics in zsm-5 zeolites," *European Journal of Molecular & Clinical Medicine*, vol. 7, no. 7, pp. 887–901, 2020.

[68] M. M. Dubinin, G. U. Rakhmatkariev, and A. A. Isirikyan, "Heats of adsorption of methanol and ethanol on high-silicon ZSM-5 zeolite," *Bulletin of the Academy of Sciences of the USSR, Division of chemical science*, vol. 38, no. 11, pp. 2419–2421, Nov. 1989.

[69] Y.-H. Yeh, C. Rzepa, S. Rangarajan, and R. J. Gorte, "Influence of brønsted-acid and cation-exchange sites on ethene adsorption in zsm-5," *Microporous and Mesoporous Materials*, vol. 284, pp. 336–342, 2019.

[70] C. G. Pope, "Adsorption of methanol and related molecules on zeolite h-zsm-5 and silicalite," *Journal of the Chemical Society, Faraday Transactions*, vol. 89, pp. 1139–1141, January 1993.

[71] J. Hunns, M. Arroyo, A. Lee, J. Escola, D. Serrano, and K. Wilson, "Hierarchical mesoporous pd/zsm-5 for the selective catalytic hydrodeoxygenation of m-cresol to methylcyclohexane," *Catal. Sci. Technol.*, vol. 6, 12 2015.

[72] G. F. Froment, K. B. Bischoff, and J. D. Wilde, *Chemical Reactor Analysis and Design*, 3rd ed. John Wiley & Sons, 2010.

[73] W. H. Weinberg, "Eley−rideal surface chemistry: direct reactivity of gas phase atomic hydrogen with adsorbed species," *Accounts of Chemical Research*, vol. 29, no. 10, pp. 479–487, 1996.

[74] A. D. M. Naught and A. Wilkinson, *Compendium of Chemical Terminology-Gold Book*, 2nd ed. International Union of Pure and Applied Chemistry (IUPAC), 1997.

[75] (2022, August) Scipy documentation — scipy v1.9.1 manual. Accessed on 05/09/2022. [Online]. Available: https://docs.scipy.org/doc/scipy/

[76] M. Huš, D. Kopač, N. S. Štefančič, D. L. Jurković, V. D. B. C. Dasireddy, and B. Likozar, "Unravelling the mechanisms of co 2 hydrogenation to methanol on cu-based catalysts using first-principles multiscale modelling and experiments †," *Cite this: Catal. Sci. Technol*, vol. 7, p. 5900, 2017.

[77] M. John, K. Alexopoulos, M.-F. Reyniers, and G. B. Marin, "Reaction path analysis for 1-butanol dehydration in h-zsm-5 zeolite: Ab initio and microkinetic modeling," *Journal of Catalysis*, vol. 330, pp. 28–45, 2015.

[78] W. Buysse, "Ab initio microkinetic modelling of bio-alcohol dehydration in zeolites: Influence of carbon number and framework topology," Master's thesis, Universiteit Gent, 2016.

[79] P. L. Houston, *Chemical kinetics and reaction dynamics*. Dover Publications, 2006, pp. 34–91.

[80] J. A. Dumesic, D. F. Rudd, L. M. Aparicio, J. E. Rekoske, and A. A. Treviño, *The Microkinetics of Heterogeneous Catalysis*. American Chemical Society, 1993.

[81] R. N. Forthofer, E. S. Lee, and M. Hernandez, "3 - descriptive methods," in *Biostatistics (Second Edition)*, second edition ed., R. N. Forthofer, E. S. Lee, and M. Hernandez, Eds. San Diego: Academic Press, 2007, pp. 21–69.

[82] K. S. Walton and R. Q. Snurr, "Applicability of the bet method for determining surface areas of microporous metal−organic frameworks," *Journal of the American Chemical Society*, vol. 129, no. 27, pp. 8552–8556, 2007, pMID: 17580944.

[83] A. Styskalik, V. Vykoukal, L. Fusaro, C. Aprile, and D. P. Debecker, "Mildly acidic aluminosilicate catalysts for stable performance in ethanol dehydration," *Applied Catalysis B: Environmental*, vol. 271, p. 118926, 8 2020.

[84] G. Yang, Y. Wang, D. Zhou, J. Zhuang, X. Liu, X. Han, and X. Bao, "On configuration of exchanged la3+ on zsm-5: A theoretical approach to the improvement in hydrothermal stability of la-modified zsm-5 zeolite," *The Journal of Chemical Physics*, vol. 119, no. 18, pp. 9765–9770, 2003.

[85] V. Kotu and B. Deshpande, "Chapter 3 - data exploration," in *Data Science (Second Edition)*, second edition ed., V. Kotu and B. Deshpande, Eds. Morgan Kaufmann, 2019, pp. 39–64.

[86] R. A. van Santen, Ed., *Physical Chemistry, Elementary Kinetics*. John Wiley & Sons, Ltd, 2017, ch. 3, pp. 59–116.

[87] T. Bligaard, J. Nørskov, S. Dahl, J. Matthiesen, C. Christensen, and J. Sehested, "The brønsted–evans–polanyi relation and the volcano curve in heterogeneous catalysis," *Journal of Catalysis*, vol. 224, no. 1, pp. 206–217, 2004.

A

Appendix A

Table A.1: Discovery library generated by making use of the FFF design. Where D1,D2 and D3 represent the chemisorption enthalpies of ethanol,ethylene and DEE, respectively. D4 and D5 represent the sticking coefficients for ethanol and ethylene and, lastly, D6 is the density of active sites.

Virtual catalyst	D1	D2	D3	D4	D5	D6
1	127.22	98.92	51.24	0.07	0.99	1.23E-06
2	120.84	91.36	54.19	0.25	0.77	1.56E-06
3	111.27	60.30	69.72	0.31	0.13	1.77E-06
4	120.32	161.64	73.37	0.03	0.22	1.96E-06
5	97.25	118.63	64.66	0.06	0.85	1.91E-06
6	57.70	113.37	61.13	0.31	0.94	1.46E-06
7	132.98	164.35	61.80	0.16	0.98	1.05E-06
8	133.31	144.46	55.16	0.05	0.60	1.74E-06
9	54.61	110.04	68.35	0.69	0.11	2.00E-06
10	44.83	43.31	53.40	0.87	0.04	1.94E-06
11	131.72	63.47	50.27	1.00	0.01	1.80E-06
12	61.30	81.78	54.34	0.18	0.18	1.73E-06
13	86.50	40.56	72.30	0.50	0.03	1.27E-06
14	73.61	45.01	61.35	0.46	0.46	1.00E-06
15	37.39	90.21	76.57	0.13	0.05	1.31E-06
16	51.69	44.22	71.29	0.06	0.14	2.43E-07

Continued on next page

Table A.1 – continued from previous page

Virtual catalyst	D1	D2	D3	D4	D5	D6
17	127.97	121.35	63.75	0.67	0.91	2.64E-07
18	103.04	160.00	54.45	0.97	0.74	9.18E-07
19	124.65	144.84	53.25	0.57	0.87	6.36E-07
20	93.86	65.15	58.94	0.65	0.72	6.74E-07
21	110.73	86.08	70.65	0.88	0.93	1.30E-06
22	129.73	90.02	59.27	0.55	0.57	1.36E-06
23	111.43	81.14	58.74	0.23	0.63	2.84E-07
24	100.29	56.34	56.53	0.60	0.48	1.88E-06
25	134.31	46.33	65.30	0.91	0.70	1.59E-06
26	128.34	81.29	67.73	0.73	0.36	1.86E-06
27	80.06	50.40	63.40	0.51	0.95	1.82E-06
28	82.73	150.99	53.64	0.39	0.23	1.44E-06
29	74.84	133.44	55.84	0.81	0.67	1.37E-06
30	76.36	96.26	60.22	0.00	0.96	2.46E-07
31	105.77	105.97	50.23	0.36	0.98	6.77E-07
32	52.42	151.83	50.91	0.32	0.67	7.45E-07
33	79.93	159.82	69.34	0.11	0.82	3.81E-07
34	75.27	55.60	53.29	0.30	0.74	3.99E-07
35	40.84	35.14	55.95	0.13	0.26	5.10E-07
36	129.32	162.53	89.89	0.49	0.66	8.91E-07
37	47.63	156.40	86.83	0.02	0.95	9.05E-07
38	87.86	101.81	58.39	0.05	0.03	7.32E-07
39	46.39	149.73	68.94	0.17	0.01	8.25E-07
40	87.41	118.16	88.06	0.12	0.54	2.73E-07
41	38.47	145.89	58.13	0.51	0.35	1.57E-06
42	71.04	98.81	82.07	0.22	0.45	1.85E-06
43	73.19	116.03	88.97	0.05	0.20	1.46E-06
44	49.06	160.78	65.61	0.89	0.89	1.18E-06
45	65.01	66.71	64.93	0.95	0.62	8.38E-07
46	50.23	92.43	69.48	0.92	0.65	3.39E-07
47	70.70	77.98	50.44	0.71	0.05	8.79E-07
48	85.33	88.38	55.70	0.74	0.41	3.75E-07
49	40.07	74.10	62.55	0.56	0.08	6.47E-07
50	69.83	164.26	63.57	0.78	0.21	5.42E-07
51	82.64	163.82	79.78	0.60	0.45	2.23E-07
52	61.93	110.95	53.89	0.61	0.70	2.03E-07
53	43.04	116.28	50.54	0.64	0.45	1.25E-06
54	60.09	158.39	60.35	0.98	0.03	1.51E-06
55	121.54	39.00	74.14	0.71	0.59	4.38E-07
56	57.35	47.07	89.07	0.96	0.96	5.09E-07
57	124.39	108.38	85.13	0.01	0.70	5.13E-07
58	116.87	42.93	80.68	0.32	0.79	2.60E-07
59	43.07	44.59	78.23	0.53	0.69	4.81E-07
60	60.24	80.09	82.90	0.15	0.90	3.50E-07
61	95.64	61.08	82.63	0.99	0.91	1.85E-06
62	85.63	111.24	89.92	0.84	0.90	1.25E-06
63	61.67	35.05	71.82	0.78	0.86	1.02E-06
64	69.32	38.71	88.71	0.53	0.26	1.92E-06
65	71.13	39.05	66.99	0.11	0.71	1.36E-06
66	54.84	82.63	74.69	0.07	0.57	1.05E-06

Continued on next page

Table A.1 – continued from previous page

Virtual catalyst	D1	D2	D3	D4	D5	D6
67	59.58	68.28	69.17	0.03	0.73	1.85E-06
68	127.94	36.89	87.41	0.35	0.82	1.76E-06
69	37.95	84.76	51.74	0.34	0.50	1.98E-06
70	77.58	39.91	50.06	0.67	0.78	1.62E-06
71	37.11	63.69	66.69	0.49	0.77	1.16E-06
72	119.88	133.94	81.92	0.11	0.92	8.05E-07
73	94.71	89.55	89.21	0.44	0.97	1.02E-06
74	129.85	123.59	77.49	0.86	0.83	1.94E-06
75	107.96	94.82	61.50	0.68	0.83	1.17E-06
76	88.63	114.24	68.16	0.46	0.69	1.68E-06
77	67.79	155.13	78.44	0.26	0.75	1.09E-06
78	66.66	143.03	85.80	0.64	0.64	1.89E-06
79	35.16	91.55	84.30	0.76	0.59	1.72E-06
80	61.77	133.66	86.24	0.24	0.79	1.59E-06
81	42.53	131.19	59.50	0.73	0.92	1.81E-06
82	39.99	164.84	76.35	0.63	0.96	1.60E-06
83	40.25	109.58	82.20	0.95	0.76	1.06E-06
84	36.21	147.52	88.25	0.69	0.74	5.65E-07
85	74.22	121.08	75.28	0.49	1.00	8.50E-07
86	62.91	134.81	77.45	0.72	0.25	1.24E-06
87	116.09	159.41	87.25	0.72	0.12	1.68E-06
88	82.11	84.06	73.71	0.98	0.31	1.53E-06
89	97.51	153.95	83.76	0.96	0.46	1.41E-06
90	134.78	89.26	83.23	0.79	0.11	9.57E-07
91	122.83	72.32	83.14	0.60	0.65	1.63E-06
92	107.65	54.85	87.80	0.88	0.34	1.99E-06
93	134.14	70.99	86.52	0.26	0.17	1.96E-06
94	98.26	75.83	80.84	0.01	0.08	1.66E-06
95	59.72	52.62	87.21	0.39	0.55	1.36E-06
96	52.61	62.44	89.24	0.59	0.01	1.50E-06
97	118.98	35.94	60.56	0.60	0.19	1.11E-06
98	132.13	75.94	57.11	0.87	0.34	2.11E-07
99	50.87	36.72	81.29	0.85	0.32	8.08E-07
100	122.53	79.58	86.26	0.90	0.06	3.87E-07
101	37.71	125.40	89.33	0.85	0.18	9.37E-07
102	59.13	124.61	83.92	0.44	0.00	6.96E-07
103	38.83	133.47	72.81	0.29	0.40	4.51E-07
104	96.06	54.70	51.09	0.21	0.02	1.19E-06
105	89.14	57.70	68.38	0.19	0.31	5.40E-07
106	72.14	65.02	77.11	0.02	0.40	3.12E-07
107	132.58	55.22	62.69	0.39	0.26	8.57E-07
108	122.06	110.43	66.16	0.41	0.45	9.39E-07
109	108.64	124.04	53.19	0.20	0.51	9.96E-07
110	115.37	148.74	59.75	0.96	0.40	3.07E-07
111	134.60	160.89	51.63	0.37	0.05	2.57E-07
112	109.26	152.63	50.71	0.50	0.08	1.99E-06
113	117.28	109.10	52.38	0.93	0.04	1.39E-06
114	78.49	131.03	81.34	0.38	0.15	1.01E-06
115	127.56	127.97	71.20	0.15	0.20	7.55E-07
116	110.01	107.61	79.22	0.54	0.31	6.00E-07

Continued on next page

Table A.1 – continued from previous page

Virtual catalyst	D1	D2	D3	D4	D5	D6
117	131.12	147.76	82.79	0.33	0.38	1.21E-06
118	105.18	141.47	64.99	0.27	0.11	1.39E-06
119	101.74	139.01	74.99	0.86	0.28	3.67E-07
120	132.79	152.22	73.42	0.81	0.53	6.44E-07